

# รายงานวิจัยฉบับสมบูรณ์

โครงการ การพัฒนาวงจรแปลงความถี่เพื่อประยุกต์ใช้ในเครื่องวิเคราะห์เครือข่าย แบบโคฮีเร้นท์

โดย รองศาสตราจารย์ คร.ประยุทธ อัครเอกฒาลิน

สัญญาเลขที่ PDF/38/42

## รายงานวิจัยฉบับสมบูรณ์

โครงการ การพัฒนาวงจรแปลงความถี่เพื่อประยุกต์ใช้ในเครื่องวิเคราะห์เครือข่าย แบบโคฮีเร้นท์

ผู้วิจัย สังกัด

รองศาสตราจารย์ คร.ประยุทธ อัครเอกฒาถิน สถาบันเทคโนโลยีพระจอมเกล้าพระนครเหนือ

สนับสนุนโดยสำนักงานกองทุนสนับสนุนการวิจัย

โครงการ การพัฒนาวงจรแปลงความถี่เพื่อประยุกต์ใช้ในเครื่องวิเคราะห์เครือข่ายแบบโคฮีเร้นท์

## บทคัดย่อ

งานวิจัยนี้เสนอวงจรเลื่อนเฟสชนิคสอดแทรกแบบใหม่ ที่ใช้โครงสร้างสายนำสัญญาณ ระนาบร่วมแบบมีกราวค์ค้านล่าง วงจรเลื่อนเฟสซึ่งใช้ไคโอควาแรกเตอร์เป็นอุปกรณ์ปรับเฟสได้ ถูกออกแบบบนแผ่นวงจรพิมพ์ใมโครเวฟ และถูกคำนวณตลอดจนจำลองการทำงานค้วยโปรแกรม คอมพิวเตอร์ วงจรเลื่อนเฟสที่นำเสนอนี้มีสมรรถนะที่สำคัญได้แก่ ค่าการสูญเสียน้อยกว่า 2 dB แบนค์วิธสูงกว่า 1 GHz และสามารถเลื่อนเฟสได้จาก 0 ถึง 360 องสา วงจรเลื่อนเฟสนี้ได้ถูกทำ การทคสอบพบว่าสามารถเลื่อนเฟสได้ครบ 360 องสา และถูกนำมาใช้เป็นวงจรเลื่อนความถี่ค้วย การขับวงจรเลื่อนเฟสค้วยแรงคันย้อนกลับรูปฟันเลื่อยที่ทำการชดเชยแล้ว (เทคนิคเซอร์โรคายน์) จากนั้นได้นำเสนอวงจรกรองผ่านแถบแบบไมโครสตริปตัวใหม่ โดยใช้โครงสร้างเรโซเนเตอร์วง เปิดแบบหน่วงคลื่นเพื่อกำจัดสัญญาณปลอมเทียมจากการเลื่อนความถี่ และในส่วนสุดท้ายของการ วิจัย จะเป็นการนำวงจรเลื่อนความถี่มาประยุกต์ใช้งานในการวัดคุณลักษณะของวงจรและอุปกรณ์ ไมโครเวฟโดยใช้เทคนิคเฮทเทอโรคายน์ ตัววัดสัญญาณสะท้อน (reflectometer) ซึ่งถูกออกแบบ และสร้างขึ้นค้วยระบบเฮทเทอโรคายน์ที่นำเสนอ เมื่อนำมาทำการทดสอบพบว่าสามารถวัดค่า สัมประสิทธิ์การสะท้อนกลับได้แม่นยำเทียบเท่าเครื่องวิเคราะห์วงจรที่จำหน่ายในท้องตลาด คำสำคัญ: วงจรเลื่อนเฟส, วงจรเลื่อนความถี่, วงจรกรองผ่านแถบ, เทคนิคเฮทเทอโรคายน์,

ตัววัคสัญญาณสะท้อน

#### **Abstract**

This research presents a new insertion type phase shifter based on a conductorbacked coplanar waveguide transmission line structure. A scale model varactor-tuned phase shifter on a microwave print circuit board has been designed and performed empirical calculations and several computer simulations. This new phase shifter shows significant performances with very low insertion loss of < 2 dB, high bandwidth of > 1 GHz, and phase change of 0-360°. The phase shifter has been tested, verifying the phase changes from 0 to 360°, and then continuously driving with the compensated sawtooth reverse bias voltage (serrodyne technique) to obtain a frequency shifting. A new class of microstrip bandpass filter with a slow-wave openloop resonator structure has been also proposed to get rid of spurious responses from Finally, the frequency shifter has been applied for RF and the shifted frequency. microwave measurement of circuit and device characteristics using a heterodyne technique. A reflectometer (one-port network analyzer) has been designed and constructed using the proposed heterodyne system. The results of measured reflection coefficients using the proposed system agree well with ones from a current commercial network analyzer.

**Keywords**: Phase shifter, frequency shifter, bandpass filter, heterodyne technique,

reflectometer

## สรุปโครงการวิจัย (Executive Summary)

งานวิจัยนี้เสนอวงจรเลื่อนเฟสชนิดสอดแทรกแบบใหม่ ที่ใช้โครงสร้างสายนำสัญญาณ ระนาบร่วมแบบมีกราวค์ค้านล่าง วงจรกรองผ่านแถบแบบไมโครสตริปชนิคใหม่โดยใช้โครงสร้าง เรโซเนเตอร์วงเปิดแบบหน่วงคลื่นเพื่อกำจัดสัญญาณปลอมเทียมจากการเลื่อนความถี่ และสุดท้าย เป็นการประยุกต์ใช้งานวงจรเลื่อนความถี่ เพื่อวัคคุณลักษณะของวงจรและอุปกรณ์ไมโครเวฟโดย ใช้เทคนิคเสทเทอโรคายน์

ผลจากการวิจัยเป็นไปตามวัตถุประสงค์ที่ตั้งไว้ทุกประการ ตลอดจนมีผลงานที่เกิดขึ้นจาก ส่วนต่างๆ ของงานวิจัยได้รับการนำเสนอในการประชุมวิชาการทั้งระดับชาติและนานาชาติ ไม่น้อย กว่า 4 เรื่อง และมีผลงานที่ตีพิมพ์ในวารสารวิชาการระดับนานาชาติ (Journal on Electronics and Telecommunications) ซึ่งเป็นวารสารที่อยู่ในฐานข้อมูล ISI และมีค่า Impact Factor อยู่ในระดับสูง เมื่อเทียบกับวารสารในสาขาเดียวกัน โดยบทความที่ได้รับการตีพิมพ์ คือ

Prayoot Akkaraekthalin and Jaruek Jantree, "Microstrip slow-wave open-loop resonator filters with reduced size and improved stopped characteristics," *ETRI Journal on Electronics and Telecommunications*, Vol.28, No.5, pp.607-614, October 2006.

การวิจัยนี้ยังสามารถขยายผลต่อไปได้อีกมาก ได้แก่ การปรับปรุงวงจรเลื่อนเฟส วงจร เลื่อนความถี่ และวงจรกรองสัญญาณ ให้มีประสิทธิภาพสูงขึ้นและขนาดเล็กลง ตลอดจนการนำไป ประยุกต์ใช้งานในด้านต่างๆ เพิ่มขึ้น โดยเฉพาะด้านการเกษตรและอุตสาหกรรมป้องกันประเทศ เป็นต้น

| ลงนาม                                    |
|--|
| (รองศาสตราจารย์ คร.ประยุทธ อัครเอกฒาลิน) |
| หัวหน้าโครงการ                           |

## 1. Introduction

All electronic phase shifters using both passive and active components (i.e. PIN diodes and FETs) are generally employed for RF and microwave communication systems in the present day. Analog phase shifters provide high resolution for small amount of phase change, whereas digital phase shifters are appropriate when a large step phase is required. These phase shifters provide low resolution of step-phase change causing low carrier and spurious sideband suppression when operating as frequency shifters. Many researchers, therefore, have developed some techniques to improve the characteristics of electronic frequency shifters by means of combination of analog and digital phase shifting techniques. This research proposes a new 360° analog phase shifter with insertion type structure using conductor-backed coplanar waveguide (CBCPW) transmission line. This phase shifter would overcome the drawbacks of the present analog phase shifters. Driving the phase shifter from 0 to 360° with time by mean of serrodyne (sawtooth) modulation results in frequency shifting that can be used as inexpensive RF and microwave sources useful for high frequency coherent measurement technique. Therefore, this research shows the application of the proposed phase shifter in frequency shifting and a coherent reflectometer system.

## 2. Theory

## 2.1 Coplanar waveguide structure

A variety of transmission line structures can be used to form phase shifters such as coaxial, microstrip and coplanar waveguide (CPW) lines. Only microstrip and coplanar wavegide are extensively utilized when fabricating monolithic microwave integrating circuits (MMICs), nevertheless, using microstrip suffers from disadvantages of high dispersion, high insertion loss, and via holes requirement. To overcome these problems, this research studies a phase shifter structure based on CPW transmission lines. Additionally, to improve the characteristics of the phase shifter, the conductor-backed coplanar waveguide (CBCPW) has been chosen due to its potential advantages over ordinary CPW, including superior mechanical strength, high power-handling capability and smaller size [1]-[2].

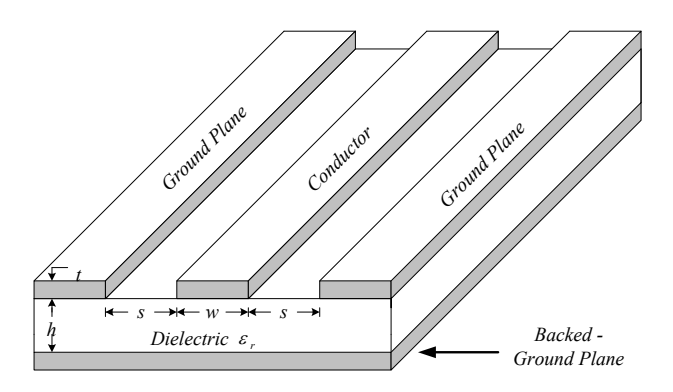


Fig.1 A CBCPW transmission line.

Figure 1 shows a structure of conductor-backed coplanar waveguide (CBCPW) consisting of a center conductor and ground planes on both sides of the print circuit board. The characteristic impedance of the CBCPW line can be calculated as [3]-[4]

$$Z_{o(line)} = \frac{60\pi}{\sqrt{\varepsilon_{re}}} \frac{1}{K(k_1)/K'(k_1) + K(k_2)/K'(k_2)}$$
(1)

where  $K(k_i)$  and  $K'(k_i)$  are the complete elliptic integrals of the first kind and its complement, respectively (when i = 1 and 2).

The ratio of K/K' can be determined as

$$\frac{K(k_i)}{K'(k_i)} = \frac{\pi}{ln\left[2\left(1+\sqrt{k_i'}\right)/\left(1-\sqrt{k_i'}\right)\right]}$$
 for  $0 \le k_i \le 0.707$  (2)

$$\frac{K(k_i)}{K'(k_i)} = \frac{1}{\pi} ln \left[ 2\left(1 + \sqrt{k_i}\right) / \left(1 - \sqrt{k_i}\right) \right]$$
 for  $0.707 \le k_i \le 1$  (3)

where  $k_i' = \sqrt{1 - k_i^2}$  and

$$k_1 = \frac{w}{w + 2s} \tag{4}$$

$$k_2 = \frac{\tanh(\pi(w/2)/2h)}{\tanh(\pi(w/2+s)/2h)}.$$
 (5)

The effective dielectric constant ( $\varepsilon_{re}$ ) of the CBCPW transmission line can be obtained as

$$\varepsilon_{r_{\sigma}} = 1 + q(\varepsilon_{r} - 1) \tag{6}$$

where

$$q = \frac{K(k_2) / K(k'_2)}{K(k_1) / K(k'_1) + K(k_2) / K(k'_2)}.$$
(7)

The phase velocity of wave on the transmission line can be calculated to be (c is the velocity of light)

$$v_{phase(line)} = \frac{c}{\sqrt{\varepsilon_{re}}}.$$
 (8)

These equations will be employed for determining the series transmission line matching at the input and output of the proposed phase shifter.

## 2.2 Analog phase shifter

A microwave phase shifter is a two-port device whose basic function is to provide a change in the phase of a microwave signal. Phase shifters can be broadly classified as being either mechanical or electronic, and also can be categorized as analog and digital phase shifters depending on the type of operation. Analog phase shifters change the phase continuously, whereas digital phase shifters allow variation of phase shift only in discrete steps, employing a sequence of binary bits to control the desired phase steps. An analog phase shifter usually provides a high phase resolution limited only by the control circuits. Typically, analog phase shifters are categorized into those which operate in passive and active modes. In passive mode, varactor diodes are usually used as tuning elements of the phase shifters [5]-[6]. Figures 2 and 3 show two types of varactor diode phase shifters used in this research. The varactor diodes provide a varying reactance to the circuit which is a function of the negative bias voltage.

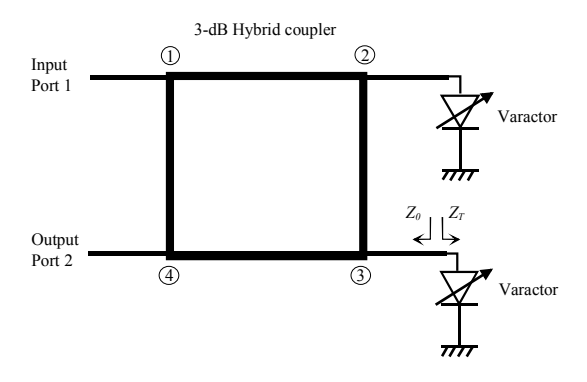


Fig. 2 Reflection type phase shifter.

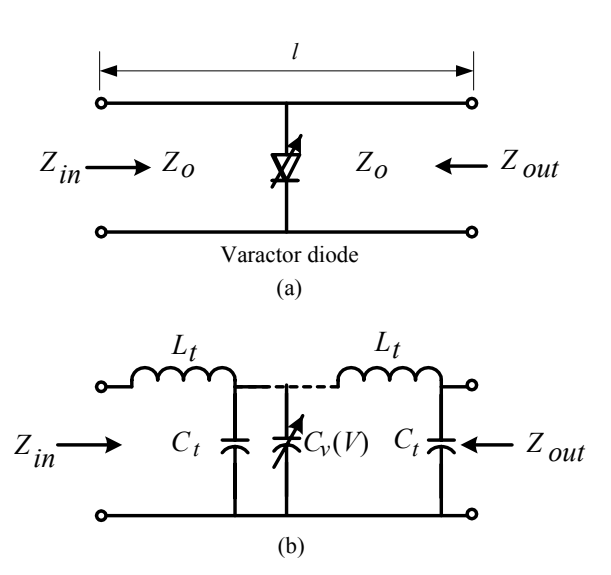


Fig. 3 Insertion type phase shifter (a) a schematic of a transmission line loaded with varactor diode and (b) its equivalent circuit.

### 2.3 Serrodyne modulation

A frequency translator or frequency shifter that changes an input RF frequency up or down by a modulation frequency is required for some applications, especially, a coherent measurement system. An ideal frequency shifter should change the original frequency  $f_o$  of a signal  $V_i$  by some modulation frequency  $f_m$  by applying a phase  $\theta =$  $2\pi f_m t$  that varies linearly with time, giving an output  $V_o = \sin(2\pi f_o t + 2\pi f_m t) = \sin(2\pi f_o t + 2\pi f_m t)$  $2\pi(f_o+f_m)t$ . This function can be realized in a continuous fashion using a rotary phase shifter, driven at a constant rate such that  $\partial \theta / \partial t = f_m$ . A frequency shifter can also be realized by means of an ideal sawtooth modulation that varies the phase linearly between zero and 360°, then flies back to zero instantaneously. This technique is called serrodyne, and is illustrated in Figure 4(a). A good frequency shifter should provide an output only at the shifted input RF frequency with minimum loss and without generating any spurious frequency. Several authors [7]-[12] have modified the serrodyne technique into a step-phase or a staircase technique to implement frequency shifters, as displayed in Figure 4(b), nevertheless, their works have been done using a coarse staircase phase function that usually suffers from insufficient carrier and spurious sideband suppression. Also, these frequency shifters are mostly realized by integrating hybrid couplers with variable capacitances or gains arising from diodes or transistors. These techniques usually limit the bandwidth of the frequency shifters. The latest-reported method of integrating fixed-delay transmission line segments, switches and drivers has enabled a 6-18 GHz digital phase shifter, which when serrodyne modulated, has given 22 dB of carrier and spurious sideband suppression [12].

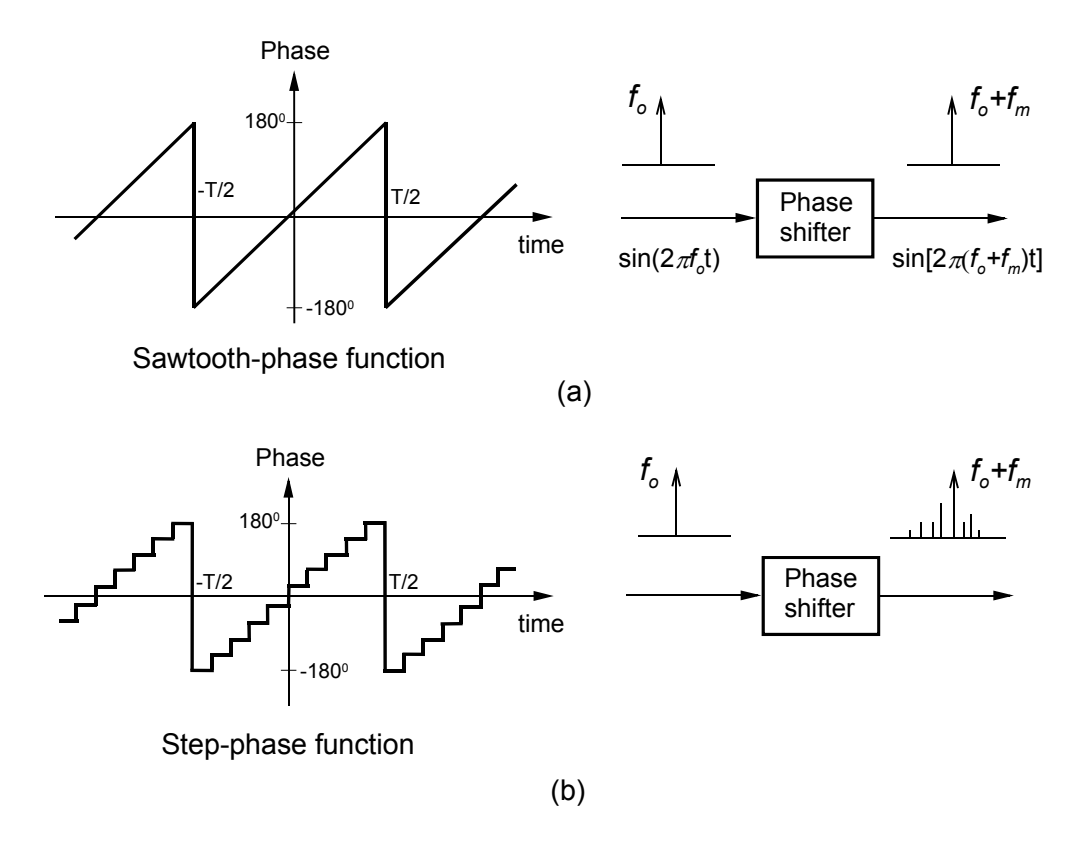


Fig. 4 Serrodyne technique (a) sawtooth modulation signal and (b) step-phase modulation signal.

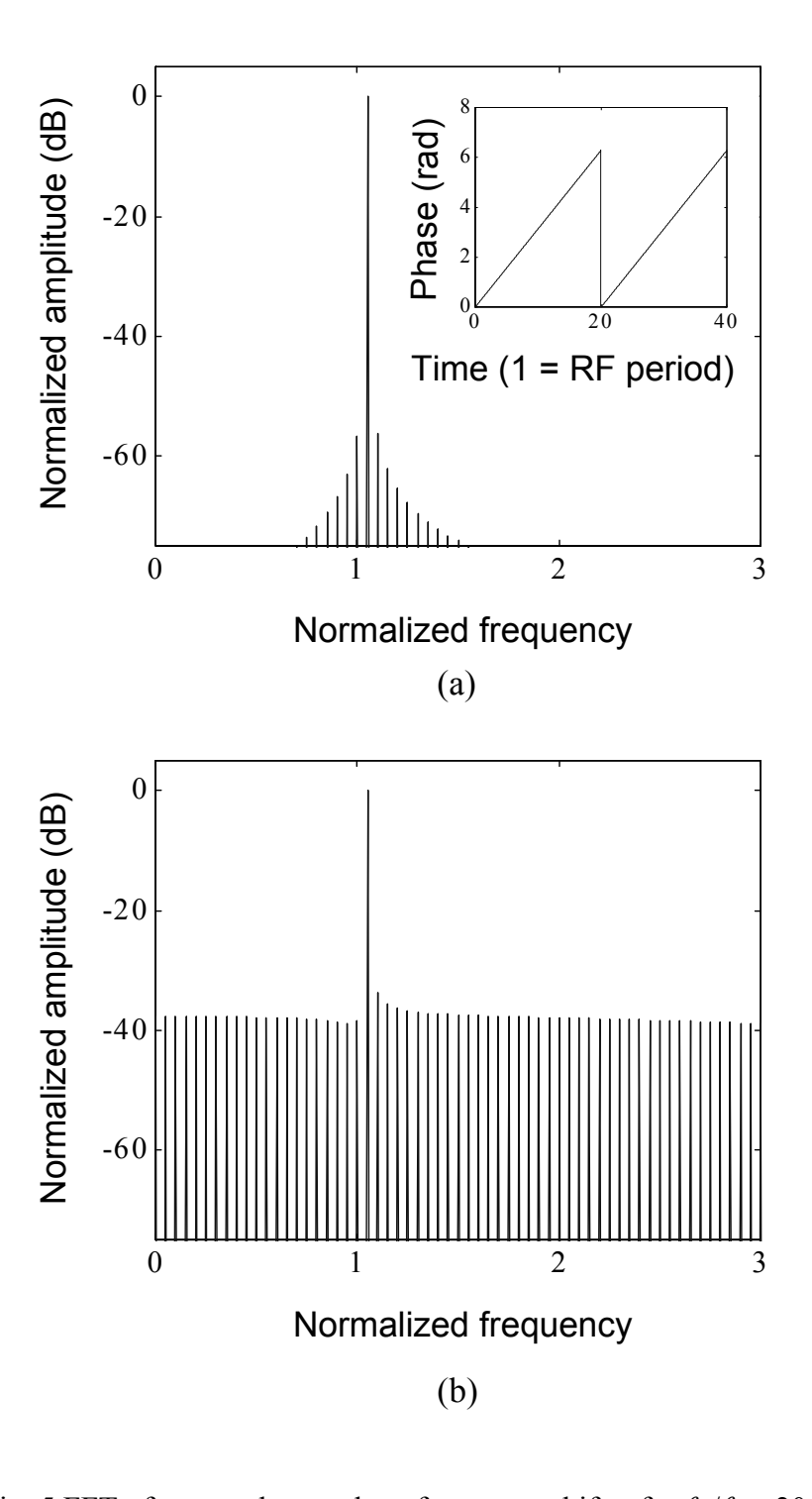


Fig. 5 FFT of sawtooth serrodyne frequency shifter for  $f_o / f_m = 20$  (a) flyback duration of 0.1% and (b) flyback duration of 1 %.

A simulation of a serrodyne frequency shifter using a continuous sawtooth scanning signal has been perform under a variety of modulation conditions to observe how the analog phase shifter would respond at increasingly higher modulation rates. Figures 5(a) and (b) show two representative results of the simulation, pointing out one limitation to achieving high-speed modulation: as the retrace transient ("flyback") time becomes increasingly signficant in the period of the sawtooth waveform, sidebands become more prominent. For example, to build an ultrawideband 500 MHz modulator with the near-ideal results of Figure 5(a) would require a 2 ps flyback in the 2 ns period. One approach to achieve such ultrawideband performance would be, in fact, to use another nonlinear transmission line (NLTL) to modulate the frequency shifter itself, since the NLTL output waveform is a sawtooth with a < 2 ps falling edge. Another approach would be to build a nonlinear control system to achieve minimum transition time during flyback. Most systems, however, do not require such high frequency modulation, though carrier and spurious sideband suppression remains important. An alternative to circuit-based approaches is to allow a longer flyback time and pause the baseband digitizing circuitry and/or Fast-Fourier Transform (FFT) calculation, allowing the circuit to fly back while ignoring the resultant spurious products that are generated (only) during this time. A similar approach we demonstrate below is to use triangle-wave phase modulation and run the FFT forwards during one cycle and backwards during the second, eliminating the retrace transient entirely.

Sidebands also result from the step-phase modulation of the phase shifter. From a Fourier series analysis of a step-phase frequency shifter [7], the normalized spectral output amplitude of the translated RF signal can be expressed as

$$\left|e_n^{\pm}\right| = \frac{\sin\frac{\pi}{N}}{(kN\pm 1)\frac{\pi}{N}} \approx \frac{1}{kN\pm 1} \tag{9}$$

where N is the number of steps in the staircase,  $n=1\pm kN$  is the spectrum number (the number of modulation frequency increments away from the input frequency  $f_o$ ),  $\pm$  indicates the upper or lower sideband, and k is an integer from 0 to  $\infty$ . If  $(n\pm 1)/N \neq k$ ,  $e_n^{\pm}=0$  (although we in fact do measure components in this regime as shown in Fig. 12). If  $(n\pm 1)/N=k$ , there will be an output at a harmonic of the modulation frequency  $f_m$ , as shown in Figure 6, when N=16. In this equation, the spurious sideband suppression level with respect to the desired output can be determined at any harmonic k. Using k=1, the maximum spurious sideband suppression level is 24.6 dBc for an 4-bit digital frequency translator (N=16). The spurious sideband suppression level will be improved by  $\sim 6$  dB for every added bit. In this work a 12-bit analog-to-digital converter has been used as an arbitrary waveform generator driving the phase shifter, so the flyback transient primarily limited the harmonic performance.

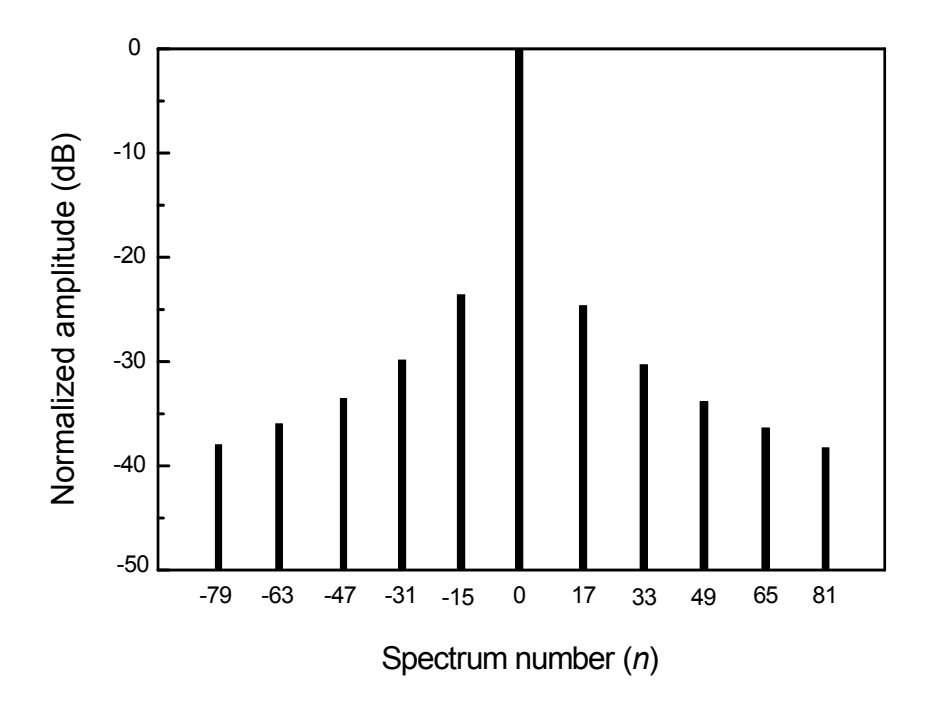


Fig.6 Spectral response of the serrodyne frequency shifter, which the spurious sidebands are resulted by the effect of 16-step (staircase) phase function .

### 2.4 Bandpass filter

In communication and instrumentation systems, RF and microwave bandpass filters are essential components usually used at front ends of transmitters and receivers. Planar filters would be preferred since they can be fabricated using printed circuit board technology with a low cost and a small size. Microstrip square open-loop resonators are proposed to form a new compact hairpin bandpass filter with the lateral size is only a one-eighth guided wavelength [13]. Further progress in size reduction is made by the proposed miniaturized hairpin resonator filters [14]. In [15] elliptic function filters are realized by U-shaped microstrip. Slow-wave and step-impedance resonator (SIR) filters are presented, resulting in size reduction and spurious frequency shifting [16]-[18].

Previously, planar cross-coupled filters have been proposed, which are mostly based on open-loop microstrip resonators [19]-[21]. The cross-coupling between nonadjacent resonators creates transmission zeros that improve the skirt rejection. In order to obtain the transmission zeros, this filter structure needs at least four resonators, however, it has been found recently that by using a 0° feed structure, two transmission zeros near the passband can be created and the stopband rejection is significantly increased. Therefore, we introduce a new class of microstrip slow-wave open-loop resonator bandpass filters based on cross-coupled and 0° feed structures. The proposed filters as shown in Figure7 include maximally flat and elliptic or quasi-elliptic function responses, resulting in not only more compact size but also a wide upper stopband (details in Appendix).

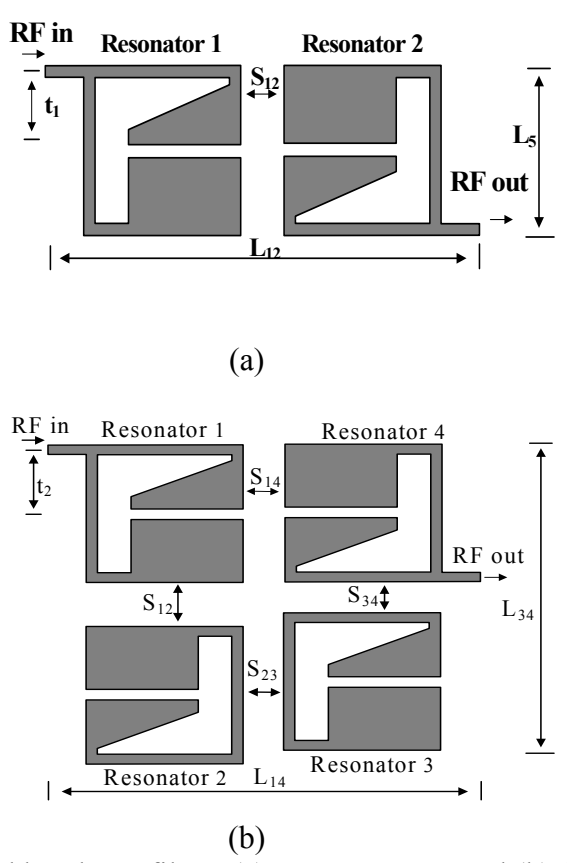


Fig. 7 The proposed bandpass filters (a) two-resonator and (b) four-resonator structures.

#### 2.5 Applications: coherent measurement

In high frequency measurement systems, two synthesizer sources are required to generate a heterodyne (coherent) output signal for characterizing a device under test (DUT). Commercial vector network analyzers (VNAs) rely on only one synthesized source and use a sampling detector, rather than using two sources and a mixer, thereby trading dynamic range for lower cost. VNAs are very accurate and can now measure network parameters for up to 100 GHz. These measurement systems are bulky, expensive, and provide only narrow instantaneous bandwidths, so their use is limited to the laboratory and to linear devices and systems. A new solution proposed here can generate a coherent signal using only one microwave synthesizer with a phase (frequency) shifter to characterize DUT, as displayed in a schematic diagram of Figure 8. This technique can enable a complete, possibly monolithic, integration of wideband network analyzers, directly addressing the need for instruments to characterize devices, circuits, and systems, as well as the growing opportunities for sensors in this regime. Driving a phase shifter with serrodyne (sawtooth) modulation results in frequency shifting that can be used with an inexpensive (ultimately integrated) microwave source to coherently convert a wideband microwave signal directly to baseband. This invention, coupled with improved directional sampling circuits [22], could enable high-performance, inexpensive, and field-capable 100 GHz vector network analysis. In addition, several other new military and commercial applications such as terahertz reflectometers which would benefit from a monolithic coherent generation/detection system [23]. This approach is the first to present a clear path to complete integration of a coherent micro- and millimeter-wave measurement system.

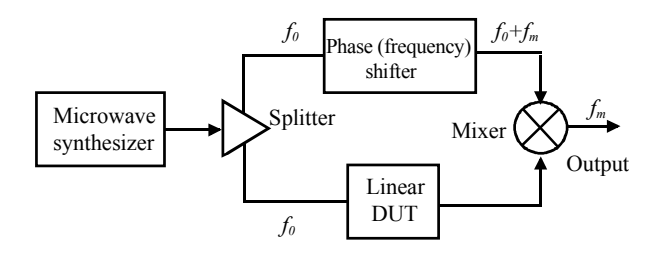


Fig.8 Coherent measurement using a phase (frequency) shifter to characterize a DUT.

A conventional microwave reflectometer consists mainly of a microwave synthesizer, a dual directional coupler and detectors. The ratio of the reflected wave and incident wave is the voltage reflection coefficient of the DUT. Reflectometers form the core of microwave network analyzers, and are typically based on power sensing (using diodes or bolometers) or coherent sampling front ends. Several techniques have been proposed to address the need for accurate reflectometry [24]. Using standard loads to calibrate a conventional reflectometer has been proposed by Hollway and Somlo [25]. This technique uses no critical components and requires no tuning adjustments, so it is simple, accurate and useful for automatic operations. The disadvantage of this technique is that the phase of the reflection coefficient cannot be measured because the detectors yield just the amplitude or power of the microwave signals. In order to obtain the phase, additional couplers or hybrids and detectors must be added. This measurement scheme was developed into a six-port reflectometer (requiring four detectors) by Engen [26]. Meanwhile, reflectometers as employed in modern commercial network analyzers use sampling front ends, which improve upon the dynamic range limitations of the six-port approaches. These could be further improved, however, by use of mixers in the front end, except that the expense of an additional microwave source is prohibitive. Homodyne reflectometers, while not commercially available, usually employ a variable-phase and reference arm derived from a single source, and they use balanced mixers as detectors. Their dynamic range is limited, however, by DC detection.

The reflectometer (one-port network analyzer) and its simplified signal flow graph are shown in Figures 9 (a) and (b). If the microwave synthesizer is matched,  $\Gamma_S = 0$ , and if the dual directional coupler is symmetrical,  $S_{31} = S_{42}$  and  $S_{32} = S_{41}$ . Solving the signal flow graph will provide the ratio of  $P_{ref}$  and  $P_{inc}$ , as shown in the following equation

$$P = \frac{P_{ref}}{P_{inc}} = \frac{B}{A} \cdot \frac{S_{32}(1 - S_{22}\Gamma_L) + S_{21}S_{31}\Gamma_L}{S_{31}(1 - S_{22}\Gamma_L) + S_{21}S_{32}\Gamma_L}.$$
 (10)

Three commercial 3.5 mm coaxial standards (matched, short and open loads) were used to calibrate the proposed reflectometer. From the above equation, substituting  $P = P_M$  for matched load ( $\Gamma_L = 0$ ),  $P = P_S$  for a short circuit ( $\Gamma_L = -1$ ),  $P = P_D$  for an open circuit ( $\Gamma_L = 1$ ), and  $P = P_L$  for an arbitrary load or DUT, and solving the equation for these conditions yield the measured reflection coefficient as

$$\Gamma_{L} = \frac{(P_{M} - P_{L})(P_{O} - P_{S})}{(P_{M} + P_{L})(P_{O} + P_{S}) - 2(P_{O}P_{S} + P_{M}P_{L})}.$$
(12)

Theoretically, using this error calibration technique, the directivity of the dual directional coupler need not be very high, and the reflectometer can be employed for accurately measuring small reflections.

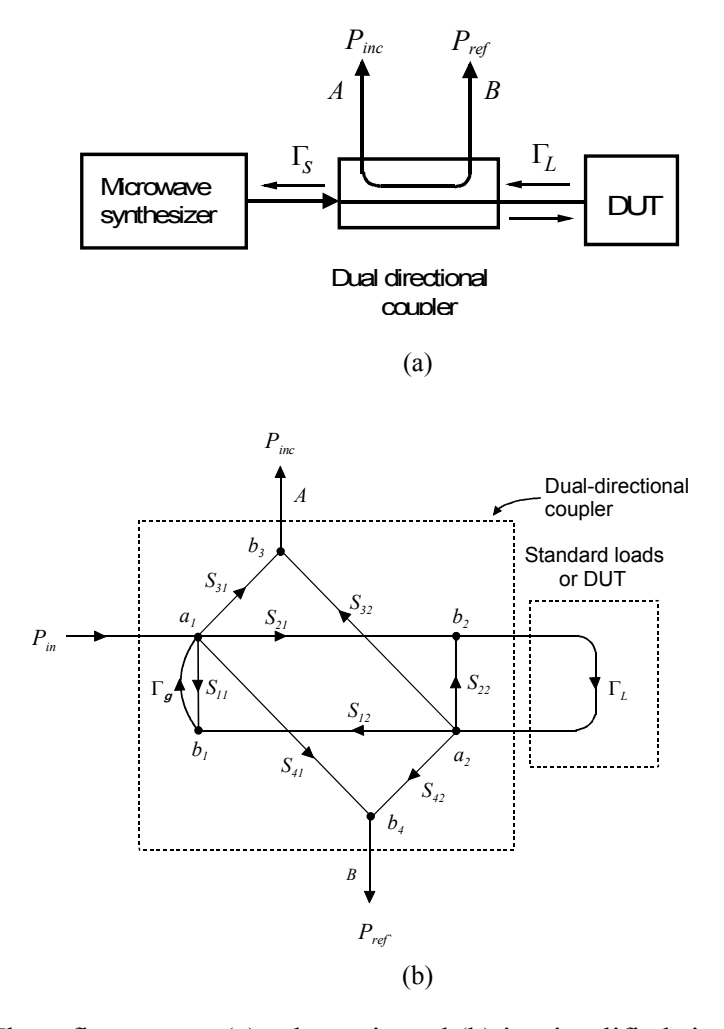


Fig. 9 The reflectometer (a) schematic and (b) its simplified signal flow graph.

## 3. Implementation and results

## 3.1 The proposed phase shifter

The proposed phase shifter has been proposed as shown in Figure 10(a). The structure is a high impedance transmission line periodically shunted by reverse biased varactor diodes to produce a synthetic structure on which the small signal propagation velocity depends on the voltage-variable capacitance. For a large signal wave, the dependence of phase velocity or delay on the voltage of the traveling wave leads to wave compression and shock wave formation because a wave travels slowly at voltage levels near zero but quickly at reverse-bias voltages where the depletion depth of the diode is large. However, when a small-signal signal propagates through the line, the wave compression or shock wave formation is not significant because the voltage differences of the traveling wave are too small for it to modulate its own phase velocity. Therefore, the proposed structure can be useful as a small-signal device in the microwave phase shifting by applying an appropriate bias voltage for a

certain phase. This phase shifter has broadband operation and low losses because its structure is distributed and low-Q. The phase shifter can be applied to frequency shifting, providing very high carrier and spurious sideband suppressions. Therefore, the proposed phase (frequency) shifter can be used in the proposed coherent system for RF and microwave measurement.

In this work, the conductor-backed coplanar waveguide (CBCPW) structure was optimally designed and built. Using a CBCPW line has several advantages compared with other types of transmission lines including lower losses, low dispersion and eliminating of air bridges. In addition, the fabrication process of a CBCPW phase shifter is also compatible with MMIC's. A microwave substrate of RO3006 with relative permittivity of  $6.15\pm0.05$  and dielectric thickness of 50 mils (1mil = 1/1000 inch) was utilized to built up the phase shifter. Varactor diodes of MSV-38 ( $R_s$ =1.7  $\Omega$  and  $C_{jo}$  = 1.26 pF) with beamlead packages from the Metelics Corp. were used as reactive elements. The simulation software named Advance Design System (ADS) was employed to analyze and optimize the proposed phase shifter. The constructed phase shifter with 14 varactor diodes is shown in Figure 10(b) (further details in Appendix).

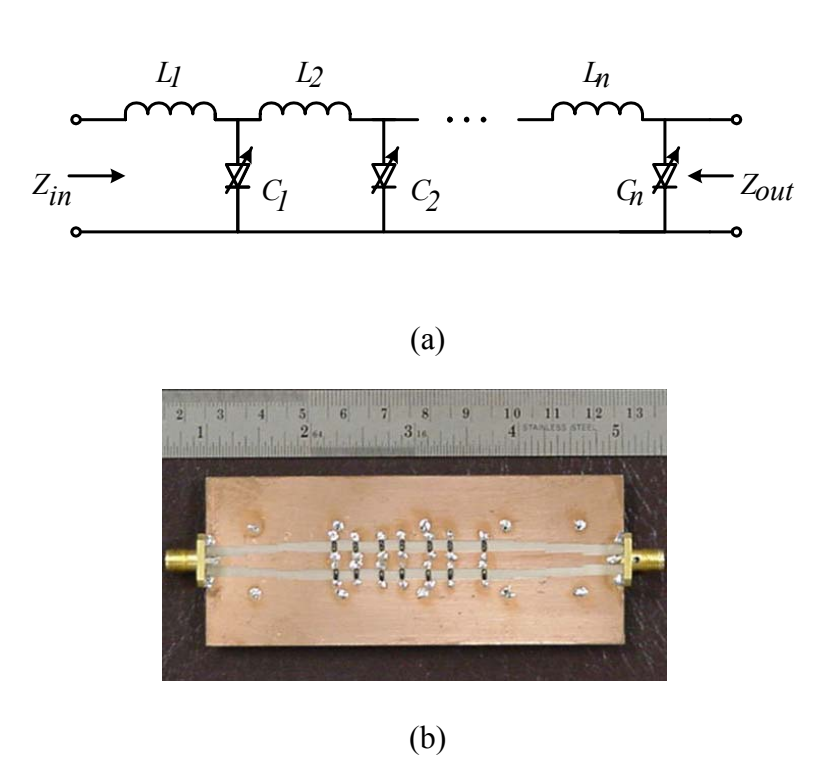


Fig.10 The proposed CPW phase shifter consisting of 14 varactor diodes (a) schematic diagram and (b) the constructed structure.

## 3.2 The proposed bandpass filter

The first filter consists of the microstrip slow—wave open-loop resonators as shown in Figure 7(a). The filter was designed on the RT/Duroid 3003 substrate with a relative dielectric constant of 3 and a thickness of 1.524 mm. In order to have a maximally flat passband bandwidth of 60 MHz (or the fractional bandwidth of FBW=3%) at  $f_0$  equal to 2 GHz. The spacing  $S_{12}$  between the resonators was adjusted to obtain the appropriate external quality factor and coupling coefficient, respectively, with the aid of an IE3D EM simulator [27]. The filter parameters were obtained in the

following:  $L_1 = 7$  mm,  $L_2 = 0.5$  mm,  $L_3 = 4.25$  mm,  $L_4 = 9$  mm,  $L_5 = 9$  mm G = 0.5 mm, and W = 0.5 mm, with spacing  $S_{12}$  equal to 1.12 mm. Figure 11 shows the fabricated filters of the proposed and conventional ones. The size of two-resonator filter is about  $0.095\lambda_{go}$  by 0.202  $\lambda_{go}$ , where  $\lambda_{go}$  is the guided wavelength of a 50- $\Omega$  line on this substrate at the center frequency. The fabricated filter was then measured on a network analyzer, with the measured and theoretical performance as shown in Figure 12. We found that the response of the proposed filter is better than the conventional one. The passband insertion loss is approximately 2.5 dB at the center frequency of 2.03 GHz, which is mainly due to the conductor loss of copper. The passband return loss is greater than 20 dB and the out-of-band rejection is better than 20 dB at the lower stopband and 20 dB at the upper stopband. The two transmission zeros are at 1.91 GHz with 42 dB rejection and 2.13 GHz with 31 dB rejection, respectively. The filter exhibits a wide upper stopband with a rejection better than 20 dB up to about 10 GHz, and the first spurious response is about 6 dB at 12.7 GHz.

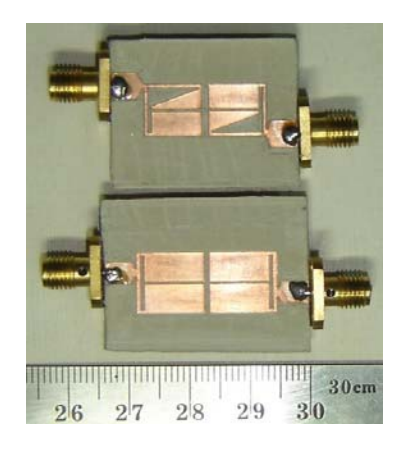


Fig. 11 The proposed bandpass filter (top) and the conventional one (bottom).

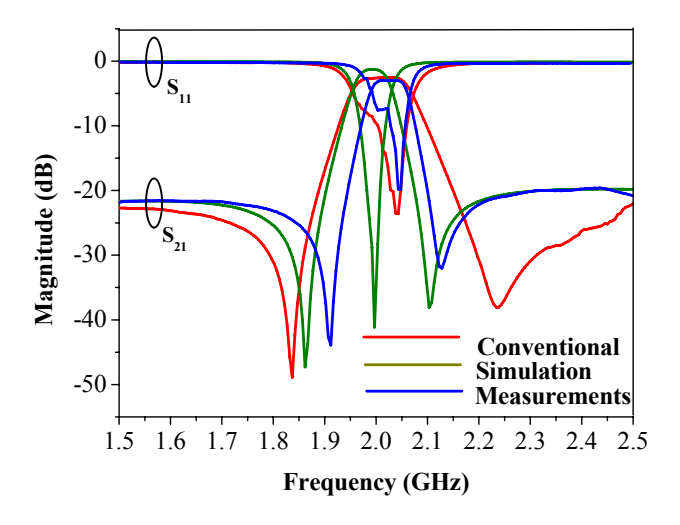


Fig. 12 Measured and simulated responses of the two-resonator bandpass filters.

The second filter is a four-resonator cross-coupled microstrip slow-wave openloop resonator filter as shown in Figure 7(b). The filter design is based on knowledge of the coupling coefficients of the three basic coupling structures, which are electric, magnetic, and mixed coupling. Therefore, the offset between resonators 2 and 3 is 1.25 mm; the spacing between the resonators has been determined as the following:  $S_{14} = 1.25$  mm,  $S_{23} = 1.5$  mm,  $S_{34} = 1.62$  mm, and  $S_{12} = 2.75$  mm. Figure 13 shows a photograph of the fabricated four-resonator bandpass filter using new microstrip slowwave open-loop resonators. In this case, the size of the filter is only 0.219  $\lambda_{go}$  by  $0.206 \lambda_{go}$ . Figure 14(a) shows the measured and theoretical data. The measured passband insertion loss is approximately 2.78 dB at the center frequency of 2.05 GHz. The passband return loss is greater than 18 dB. The out-of-band rejection is better than 22 dB at the lower stopband and 20 dB at the upper stopband. In Figure 14(b), the filter exhibits a wide upper stopband with a rejection better than 25 dB up to about 10.5 GHz. It can also be clearly seen that there is an unnatural dip in the response at  $f_I$ around 6 GHz. The reason for this dip is that the bandstop characteristic of the asymmetrical parallel coupled-line of the proposed resonator causes superior suppression of the spurious response as previously discussed (further details in Appendix).

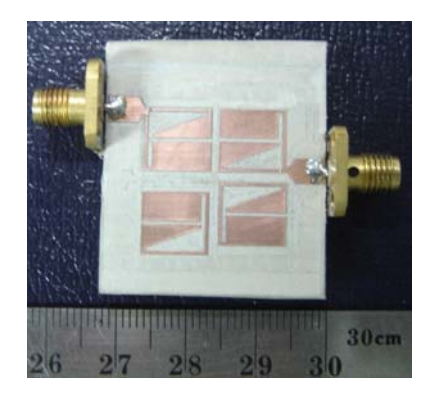


Fig. 13 The fabricated four-resonator bandpass filter.

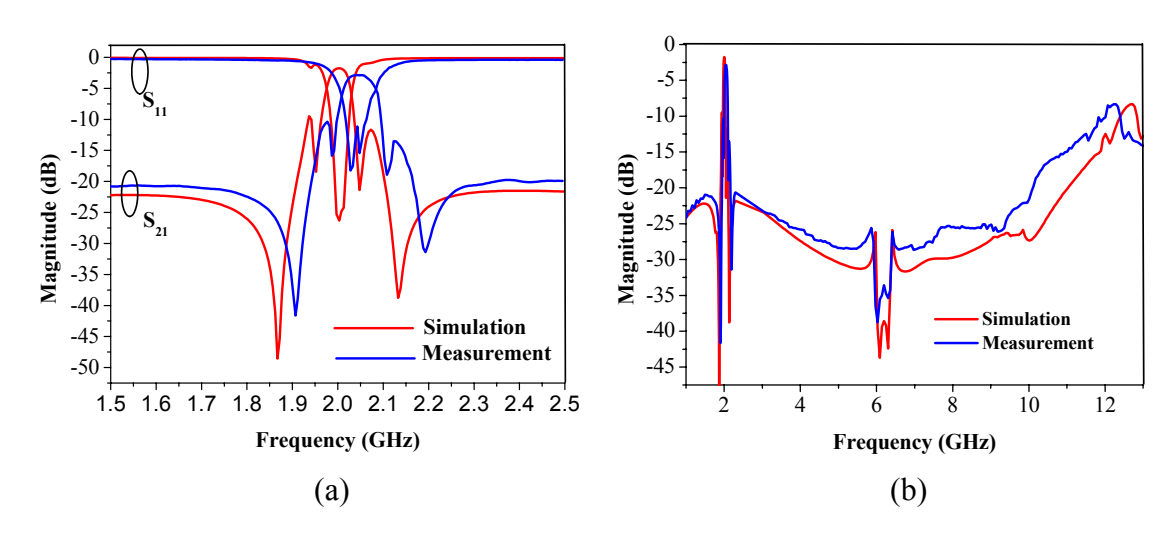


Fig.14 Measured and simulated responses of the four-resonator filter (a) passband response and (b) wideband response.

## 3.2 Experimental result: frequency shifting

The phase shifter was then tested to verify that its phase angle (delay time) can be varied from 0 to 360° as a result of the delay time compared with the simulation shown in Figure 15. A good frequency shifter should provide an output of only the shifted carrier frequency with minimum power loss and without generating spurious frequencies. One way to create a frequency shifter is to use a phase shifter as a phase modulator. When the phase angle of an input RF signal is varied linearly with time, a frequency of the resultant output signal is translated to a new frequency.

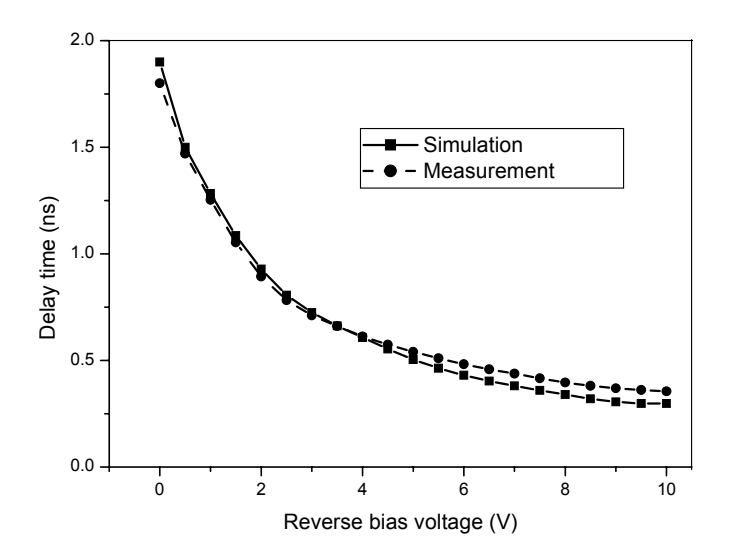


Fig. 15 Simulated and measured delay time of the proposed phase shifter.

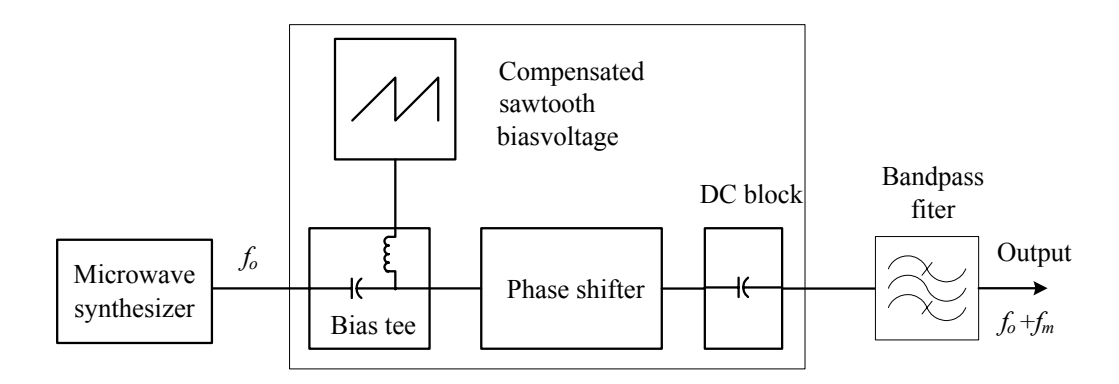


Fig. 16 Experimental circuit of frequency shifting.

An ideal frequency shifter can be accomplished by using a phase shifter controlled by a linear phase function of modulation frequency. However, this can be practically achieved by driving a phase shifter with a periodic sawtooth phase function, varying the phase linearly between 0 and  $360^{\circ}$ , then flying back to zero instantaneously. This phase modulation method is also known as the serrodyne technique as discussed. In this research, the serrodyne modulation was utilized with the proposed phase shifter. Figure 16 shows the experiment set up for verifying the frequency shifter performance. The phase shifter was continuously driven with the compensated sawtooth reverse bias voltage at a frequency of  $\sim 100~{\rm Hz}$ , resulting in a frequency shifting. The signal spectrum from the bandpass filter output as shown in Figure 17 taken from a spectrum analyzer confirms that the translated (frequency shift) signal is a nearly pure sinusoidal waveform suitable for high performance coherent measurement systems.

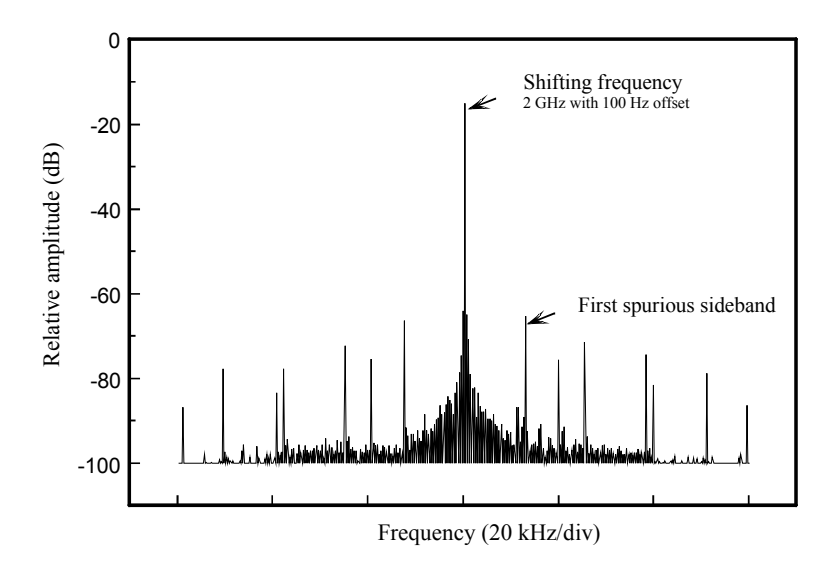


Fig. 17 Measured RF spectrum of the proposed frequency shifter.

## 3.3 Experimental result: coherent measurement

The proposed phase shifter was utilized as a frequency shifter in a coherent reflectometer system (Figure 18). The signal from the microwave synthesizer was split into the frequency shifter input and mixer LOs. A dual-directional coupler (HP 11692D) was used to couple the incoming signal from the frequency shifter and the reflected signal from a DUT. These signals were fed into mixers (RF), resulting in downconverted ~100 Hz intermediate frequency (IF). The spectrum of the IF signals (20 periods) were taken by fast Fourior transform (FFT) using a LabVIEW program on the microcomputer, from which the amplitude and phase of the incident (channel 1) and reflected (channel 2) waves were obtained. The calculation of complex reflection coefficient was then performed by the microcomputer. The measurement of 25  $\Omega$  loads from 1 to 3 GHz by using the calibrated reflectometer are shown in Figure 19. These results agree very well with ones from a commercial network analyzer (HP 8720D).

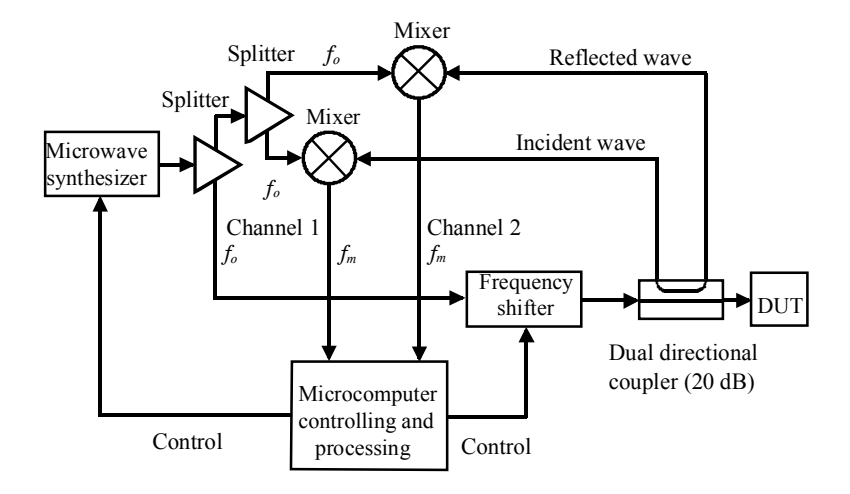


Fig.18 The coherent reflectometer system.

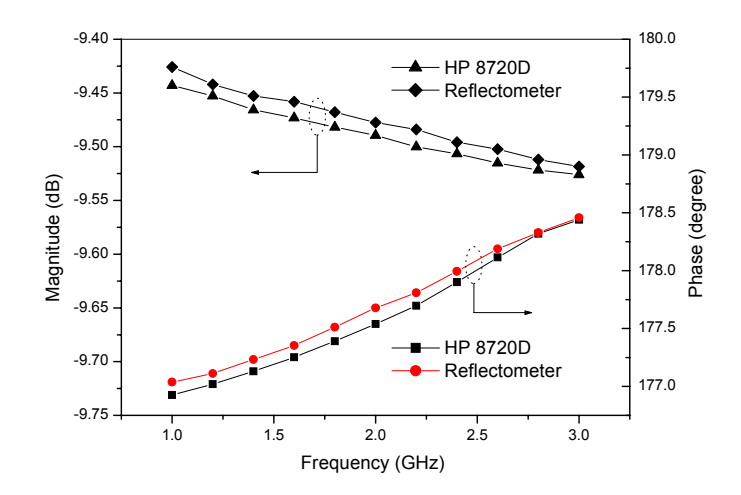


Fig. 19 Measurement of reflection coefficient for a 25  $\Omega$  load.

## 4. Conclusions

A new phase shifter with a conductor-backed coplanar waveguide (CBCPW) structure has been proposed. This phase shifter can be utilized to generate a shifted frequency by using the serrodyne technique. To generate a high quality RF shifted frequency, the new bandpass with slow-wave open-loop resonators has been also Using the phase shifter and the heterodyne (coherent) technique for microwave measurement, it has been proofed that the system is a very high accuracy, high stability and potentially low-cost system. This new approach is expected to strongly support the future RF and microwave measurement systems because it offers a clear path toward complete integration into MICs and MMICs. It will also have significant applications in other advanced instrumentation and wireless communication systems.

## Acknowledgment

This work has been supported by the Thailand Research Fund (TRF) under the grant number PDF/38/42.

## References

- [1] K. W. Tan and S. Uysal, "Analysis and design of conductor-backed asymmetric coplanar waveguide line using conformal mapping techniques and their application to end-coupled filters," *IEICE Trans. on Electron.*, vol.E82-C, pp.1098-1103, Jul. 1999.
- [2] C. H. Wu and S. Uysal, "A new systematic and efficient method of analysis for conductor-backed coplanar-waveguide directional couplers," *IEEE Trans. on Microwave Theory and Tech.*, vol.MTT-47, pp.1127-1131, Jul. 1999.
- [3] G. Ghione and C. Naldi, "Parameters of coplanar waveguide with lower ground plane," *Electron. Lett.*, vol.19, pp.734-735, Sep. 1983.
- [4] K. C. Gupta, R. Garg, I. Bahl and P. Bhartia, Microstrip Lines and slotlines, 2<sup>nd</sup> edition, Norwood, MA, Artech House, 1996.
- [5] D.E. Dawson, A.L Conti, S.H. Lee, G.F. Shade, and L.E. Dickens, "An analog X-band phase shifter," *IEEE Microwave Millimeter-Wave Monolithic Circuit Symp.*, pp.6-10, 1984.
- [6] E.C. Niehenke, V.V. DiMarco, and A. Friedberg, "Linear analog hyperabrupt varactor diode phase shifters," *IEEE MTT-S Microwave Symp. Digest*, pp.657-660, 1985.
- [7] J.S. Jaffe and R.C. Mackey, "Microwave frequency translator," *IEEE Trans. Microwave Theory and Tech.*, vol.13, pp.371-378, 1965.
- [8] G. Klein and L. Dubrowsky, "The DIGILATOR, a new broadband microwave frequency translator," *IEEE Trans. Microwave Theory Tech.*, vol.15, pp.172-179, 1967.
- [9] S.R. Mazumder, T.L. Tsai, and W.C. Tsai, "A frequency translator using dual-gate GaAs FETs," *IEEE MTT-S Digest*, pp.346-348, 1983.
- [10] S. Lucyszyn, I.D. Robertson, and H. Aghvami, "24 GHz serrodyne frequency translator using a 360 degree analog CPW MMIC phase shifter," *IEEE Microwave Guided Wave Lett.*, vol.4, pp.71-73, 1994.
- [11] L.J. Kushner, G.V. Andrews, W.A. White, J.B. Delaney, M.A. Vernon, M.P. Harris, and D.A. Whitmire, "An 800 MHz monolithic GaAs HBT serrodyne modulation," *IEEE Solid-State Circuits*, vol. 30, pp.1041-1049, 1995.
- [12] S. Mazumder and C. Isham, "Frequency translation by phase shifting," *Appl. Microwave & Wireless*, pp.144-152, 1995.
- [13] J.S. Hong and M.J. Lancaster, "Coupling of microstrip square open-loop resonators for cross- coupled planar microwave filter," *IEEE Trans. Microwave Theory Tech.*, vol.44, pp.2099-2109, Dec. 1996.
- [14] J.T. Kuo, M.J. Maa, and P.H. Lu, "A microstrip elliptic function filter with compact miniaturized hairpin resonators" *IEEE Trans. Microwave Theory Tech.*, vol.10, pp.94-95, Mar. 2000.
- [15] J.S. Hong and M.J. Lancaster, "Cross-coupled microstrip hairpin-resonator filters," *IEEE Trans. Microwave Theory Tech.*, vol.46, pp.118-122, Jan. 1998.
- [16] M. Makimoto and S. Yamashita, "Bandpass filters using parallel coupled stripline stepped impedance resonators," *IEEE Trans. Microwave Theory Tech.*, vol.MTT-28, pp.1413-1417, 1980.
- [17] M. Sakawa, K. Takahashi, and M. Makimoto, "Miniaturized hairpin resonator filters and their application to receiver front-end MIC's," *IEEE Trans. Microwave Theory Tech.*, vol.37, pp.1991-1997, Dec. 1989.

- [18] J.S. Hong and M.J. Lancaster, "Theory and experiment of novel microstrip slow—wave open-loop resonator filters," *IEEE Trans. Microwave Theory Tech.*, vol.45, pp.2358-2365, Dec. 1997.
- [19] R. Levy, "Filters with Single Transmission Zeros at Real or Imaginary Frequencies," *IEEE Trans. Microwave Theory Tech.*, vol. MTT-24, Apr. 1976, pp. 172-181.
- [20] J.S. Hong and M.J. Lancaster, "Couplings of Microstrip Square Open-Loop Resonators for Cross-Coupled Planar Microwave Filters," *IEEE Trans. Microwave Theory Tech.*, vol. 44, no. 12, Dec. 1996, pp. 2099-2109.
- [21] J.S. Hong and M.J. Lancaster, "Design of Highly Selective Microstrip Bandpass Filters with a Single Pair of Attenuation Poles at Finite Frequencies," *IEEE Trans. Microwave Theory and Tech.*, vol. 48, no. 7, July 2000, pp. 1098-1107.
- [22] R. Y. Yu, M. Reddy, J. Pual, S. T. Allen, M. Case, and M. J. W. Rodwell, "Millimeter-wave on-wafer waveform and network measurements using active probes," *IEEE Trans. Microwave Theory Tech.*, vol.43, pp.721-729, 1995.
- [23] J. S. Bostak, D. W. van der Weide, D. M. Bloom, B. A. Auld, and E. Ozbay, "All electronic terahertz spectroscopy system with terahertz free-space pulses," *J. Opt. Soc. Am. B*, vol.11, pp.2561-2565, 1994.
- [24] F. C. DeRonde, "A precise and sensitive X-band reflectometer providing automatic full-band display of reflection coefficient," *IEEE Trans. Microwave Theory Tech.*, vol.13, pp.435-440, 1965.
- [25] D. L. Hollway and P. I. Somlo, "A high-resolution swept-frequency reflectometer," *IEEE Trans. Microwave Theory Tech.*, vol.17, 1969.
- [26] G. F. Engen, "A (historical) review of the six-port measurement technique," *IEEE Trans. Microwave Theory Tech.*, vol.45, pp.2414-2417, 1997.
- [27] Zeland Software, Inc., IE3D manual, New York, 2004.

## **APPENDIX**

## **Publications from this research**

## **Proceedings**

- 1. Prayoot Akkaraekthalin, Somrat Nimyen, and Vech Vivek, "Conductor-backed coplanar waveguide hybrid for varactor-tuned phase shifting," *The 3<sup>rd</sup> International Symposium on Wireless Personal Multimedia Communications*, Bangkok, pp.953-957, Nov. 12-15, 2000.
- 2. Warunee Dangchom, Prayoot Akkaraekthalin, and Vech Vivek, "A novel insertion type phase shifter using conductor-backed coplanar waveguide," *The 23<sup>rd</sup> Electrical Engineering Conference (EECON-23)*, Chiang Mai, pp.333-336, Nov. 23-24, 2000.
- 3. Prayoot Akkaraekthalin, Chachawan Sawangnate, and Vech Vivek, "Conductor-backed coplanar waveguide directional coupler and its use for a varactor-tuned 90° phase shifter," *The Asia-Pacific Conference on Circuits and Systems*, Tianjin, China, pp.525-528, Dec. 4-6, 2000.
- 4. Prayoot Akkaraekthalin, "A novel analog phase shifter for microwave measurement," *The Asia-Pacific Symposium on Broadcasting and Communications*, Bangkok, pp.70-73, Dec. 21-23, 2000.

## **International Journal**

1. Prayoot Akkaraekthalin and Jaruek Jantree, "Microstrip slow-wave open-loop resonator filters with reduced size and improved stopped characteristics," *ETRI Journal on Electronics and Telecommunications*, Vol.28, No.5, pp.607-614, October 2006.

# Microstrip Slow-Wave Open-Loop Resonator Filters with Reduced Size and Improved Stopband Characteristics

Prayoot Akkaraekthalin and Jaruek Jantree

This paper presents a new class of microstrip slow-wave open-loop resonator filters with reduced size and improved stopband characteristics. A comprehensive treatment of both ends loaded with triangular and rectangular ends is described, leading to the invention of a microstrip slow-wave open-loop resonator. Two-resonator and four-resonator bandpass filters are designed at the operating frequency of about 2 GHz, and a bandwidth of 60 MHz. The size of the slow-wave open-loop resonator is optimized from the standpoint of the unloaded Q-factor. The filters are not only compact in size due to the slow-wave effect, but also have a wider upper stopband resulting from the dispersion effect. The filter designs of this type are described in details. The experimental results are demonstrated and discussed.

Keywords: Microstrip slow-wave open-loop resonator, bandpass filter.

## I. Introduction

Radio frequency and microwave planar bandpass filters are presently required in a wide variety of applications of wireless communication systems [1]. Recent advances in hightemperature superconducting (HTS) circuits and microwave monolithic integrated circuits (MMIC) have additionally stimulated the development of various planar filters, especially narrow-band bandpass filters which play an important role in modern communication systems [2]-[6]. Currently, filters with compact size which suppress spurious sidebands and have wider upper stopbands are necessarily required for several wireless communication systems. However, most of the planar bandpass filters built on microstrip structures are large in size and their first spurious resonance frequencies appear at  $2f_0$  and  $3f_0$ , where  $f_0$  is the center frequency, which maybe closed to the desired frequencies. The half-wavelength resonators inherently have a spurious passband at  $2f_0$ , while quarter-wavelength resonator filters have the first spurious passband at  $3f_0$ , but they require short-circuit connections with via holes, which are not quite compatible with planar fabrication techniques. Previously, most studies proposed techniques for the suppression of spurious passbands of the filters using microstrip parallelcoupled lines. Parallel-coupled microstrip filters with overcoupled end stages have been proposed to extend the electrical length of the odd mode to compensate the difference in the phase velocities [7]. The wiggly-line microstrip filter using a continuous perturbation of the width of the coupled lines following a sinusoidal law has been studied [8]. Parallelcoupled microstrip filters with the width of slots in the ground

Manuscript received Jan. 12, 2006; revised July 06, 2006.

This work was supported by the Thailand Research Fund under grant number PDF/38/2542, the National Electronics and Computer Technology Center (NECTEC), the National Science and Technology Development Agency (NSTDA), Thailand, under the grant number 13/2547.

Prayoot Akkaraekthalin (phone: +662 9132500, email: prayoot@kmitnb.ac.th) and Jaruek Jantree (email: jaruekja@hotmail.com) are with Department of Electrical Engineering, King Mongkut's Institute of Technology, Bangkok, Thailand.

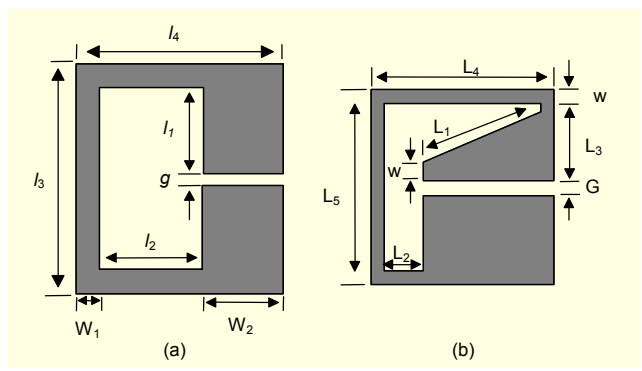


Fig. 1. (a) A conventional resonator and (b) the proposed microstrip slow-wave open-loop resonator.

plane adjusted to compensate unequal modal electrical lengths to obtain spurious suppression have been proposed [9], [10].

The substrate suspension structure has been designed to substantially speed up the even-mode phase velocity to make the modal phase velocities equal for the suppression of spurious bands [11]. These published microstrip-coupled line filters have some key drawbacks. All of these filters are very long due to their straight structures, especially when the filter order becomes high. The filters in [9] and [10] need groundplane apertures and that in [11] needs a suspended substrate, which increases the complexity and cost. Besides, many other proposed filters use stepped impedance resonators (SIR) to shift away the first higher order resonance frequency [12]-[14]. However, the step impedance method is to move, not to suppress, the first spurious band and sometime a large impedance stepping ratio is required and makes the layout of the filter difficult. Capacitively-loaded transmission lines as slow-wave open-loop resonators and SIR have been found advantageous for controlling the spurious bands, however, their spurious responses are still large [12]-[16].

Cross-coupled resonator filters are traditionally realized using waveguide cavities or dielectric resonators, which are bulkier than planar structures. Previously, planar cross-coupled filters have been proposed, which are mostly based on openloop microstrip resonators [17]-[19]. The cross-coupling between nonadjacent resonators creates transmission zeros that improve the skirt rejection. In order to obtain the transmission zeros, this filter structure needs at least four resonators, however, it has been found recently that by using a 0° feed structure, two transmission zeros near the passband can be created and the stopband rejection is significantly increased [14]. Therefore, we introduce a new class of microstrip slowwave open-loop resonator bandpass filters based on crosscoupled and 0° feed structures. The proposed filters include maximally flat and elliptic or quasi-elliptic function responses, resulting in not only more compact size but also a wide upper

stopband.

In section II, a brief comparison of the proposed microstrip slow-wave open-loop resonators and the conventional one is made in view of their sizes, coupling characteristics, and fundamental and first spurious resonance frequencies. In section III, we describe the size optimization of the proposed resonator from the standpoint of the unloaded Q-factor. The designs and measured results of both a two-resonator filter and a four-resonator cross-coupling filter using the proposed resonators are described in detail in section IV. Finally, our conclusions are given in section V.

## II. Comparison of the Conventional and Proposed Microstrip Slow-Wave Open-Loop Resonators

Figure 1(a) shows a conventional microstrip hairpin resonator [14]. The proposed microstrip slow-wave open-loop resonator composed of a microstrip line loaded with triangular and rectangular ends is shown in Fig. 1(b). The slow-wave behavior is caused by the capacitive loading effect from both ends. The resonance responses of the conventional and proposed microstrip slow-wave open-loop resonators are computed by using IE3D [20], a commercial electromagnetic simulator. An RT/Duroid 3003 substrate, which has a given dielectric constant of 3 and a thickness of 1.524 mm is used, resulting in curves as given in Fig. 2. The resonance responses are obtained from the microstrip slow-wave open-loop resonators with the same size. It can be noticed that the proposed resonator has a resonance frequency of 2 GHz, compared to 2.45 GHz of the conventional one. This means that the proposed microstrip resonator can be made smaller than the conventional structure when they resonate at the same frequency. The coupling coefficients are also computed by using IE3D simulation software. Figure 3 shows a magnetic coupling. The variation of coupling coefficient K versus the distance S between two resonators is drawn by dashed and solid lines for the conventional resonators and the proposed resonators, respectively. It is seen that the proposed resonators have smaller K than conventional resonators. This can be explained by the fact that both the conventional and proposed resonators have electric and magnetic coupling, but the magnetic couplings are dominant. The magnetic fringing fields of the conventional resonators are stronger near the center of the resonators, but the magnetic fringing fields of the proposed microstrip resonators distribute asymmetrically at the resonator line. Therefore, both the size and the coupling property of a resonator, as well as the specifications of a filter, need to be considered in choosing resonators. Roughly speaking, if a narrowband filter is designed, smaller coupling coefficients between resonators will be required [2], therefore the proposed

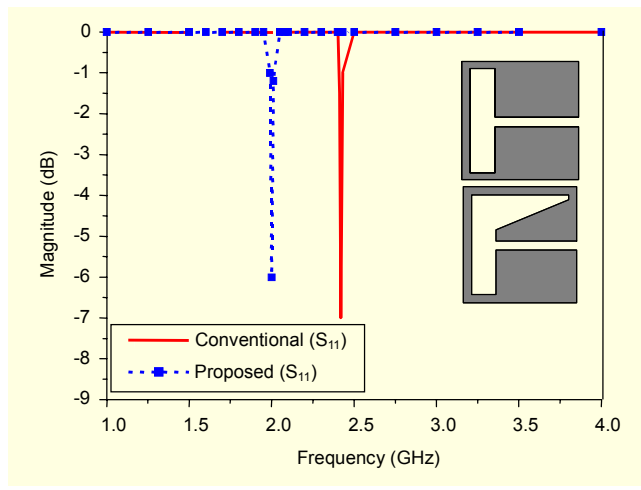


Fig. 2. Performance of the conventional resonator with  $l_1 = 4.2$  mm,  $l_2 = 0.5$  mm,  $l_3 = 9$  mm,  $l_4 = 9$  mm,  $W_1 = 0.5$  mm,  $W_2 = 8$  mm, and g = 0.5 mm; and the proposed microstrip slow-wave open-loop resonator with  $L_1 = 7$  mm,  $L_2 = 0.5$  mm,  $L_3 = 4.25$  mm,  $L_4 = 9$  mm,  $L_5 = 9$  mm, W = 0.5 mm, and G = 0.5 mm.

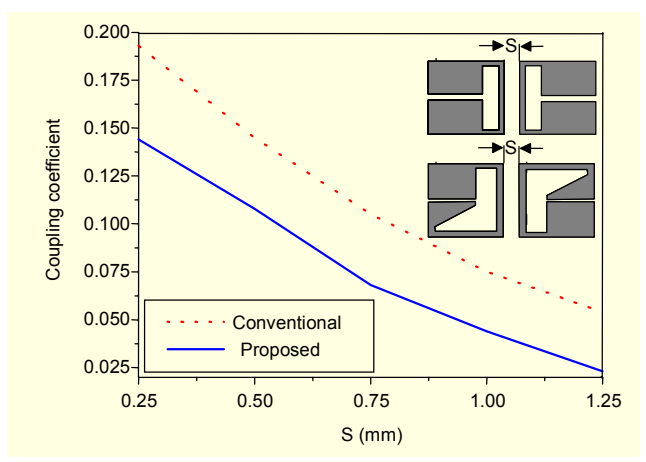


Fig. 3. Variation of the coupling coefficient K versus the distance S between two coupled resonators of the conventional resonator with  $l_1=4.87$  mm,  $l_2=0.5$  mm,  $l_3=10.75$  mm,  $l_4=10.75$  mm,  $W_1=0.5$  mm,  $W_2=9.75$  mm, and g=0.5 mm; and the proposed resonator with  $L_1=7$  mm,  $L_2=0.5$  mm,  $L_3=4.25$  mm,  $L_4=9$  mm,  $L_5=9$  mm, W=0.5 mm, and G=0.5 mm,

microstrip slow-wave open-loop resonators are preferred; if a wideband response is required, it may be preferable to choose conventional resonators.

#### III. An Optimized Resonator and Its Bandstop Characteristic

#### 1. An Optimized Resonator

The size of the proposed microstrip slow-wave open-loop resonator has been optimized from the standpoint of the unload

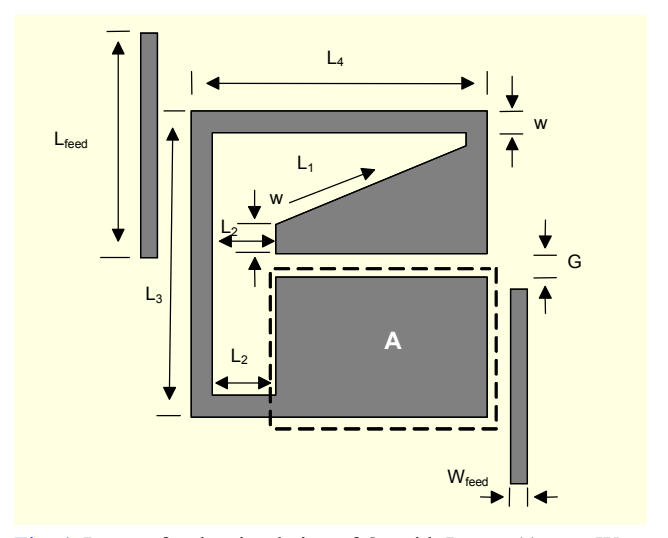


Fig. 4. Layout for the simulation of  $Q_u$  with  $L_{feed} = 11$  mm,  $W_{feed} = 0.5$  mm, and  $L = L_3 + L_4$  mm when  $L_3 = L_4$ .

Q-factor of the resonator with an IE3D simulator. We assume that the conductivity of the metal is  $\sigma = 5.8 \times 10^7$  [S/m], the dielectric loss tangent is  $\tan \delta = 0.0013$ , the dielectric constant is 3, and the thickness is 1.524 mm. In Fig. 4, the line width W and gap G are varied, while the lengths L and L<sub>2</sub> have been adjusted so that the resonance frequency of the microstrip slow-wave open-loop resonator  $f_0$  is equal to 2 GHz. The unloaded Q-factor  $Q_u$  can be calculated by the following equation [21]:

$$Q_u = \frac{Q_L}{1 - 10^{-\frac{L_0}{20}}},\tag{1}$$

where  $Q_L$  is the loaded Q-factor and  $L_0$  is the insertion loss in decibels of the resonance frequency that is obtained from the simulated result of the resonator. The resonator layout used for our simulation is shown in Fig. 4. Figure 5(a) shows the variation of the unloaded Q-factor  $Q_u$  against the line width W and the gap G It is seen that as the width of gap G increases, the unloaded Q-factor  $Q_u$  will increase and saturate when the width W is a large number, however, the area of the resonator increases. The key area of the resonator is assumed to be A, since when adjusting width W and gap G, area A of the resonator will be affected more than other parts. We obtain  $Q_u/A$  by dividing the unloaded Q -factor  $Q_u$  by occupation area A, as shown in Fig. 5(b). The higher the  $Q_u / A$  value is, the higher the Q -factor  $Q_u$  for each unit area is. In other words, the area of the resonator that has the same Q-factor  $Q_u$  can be reduced, so we can reduce the area of the filter without increasing its insertion loss. The point is, G = 0.5 mm and W =0.5 mm, seem to be optimum because the  $Q_u/A$  value is very high as we can clearly see in Fig. 5(b).

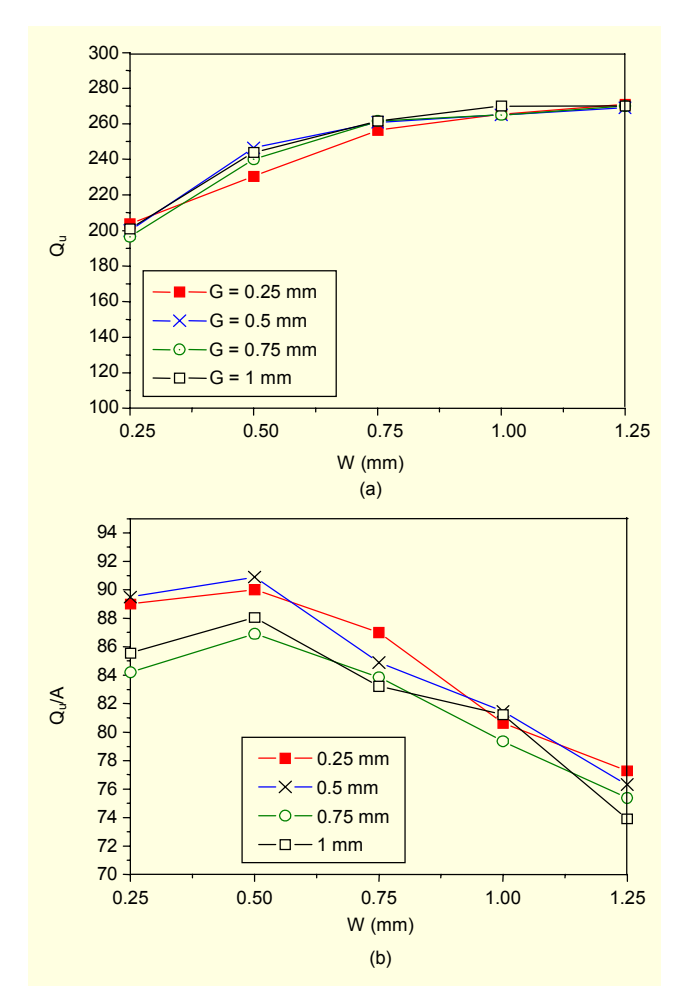


Fig. 5. Variation of  $Q_u$  and  $Q_u/A$  with the W and G of the proposed slow-wave open-loop resonator.

#### 2. Bandstop Characteristic for Spurious Suppression

The proposed microstrip slow-wave open-loop resonator has been optimized, resulting in the final dimensions as shown in the previous subsection. The resonator has an inherent bandpass characteristic with the fundamental resonance frequency of 2 GHz and the first spurious resonance frequency of about 6 GHz. The loading capacitances at the open-ends of the proposed resonator have been further studied in detail. These loading capacitance parts are formed in an asymmetrical parallel-coupled line structure as shown in Fig. 6. The IE3D has been employed to evaluate the characteristics of the asymmetrical parallel-coupled line section by using differential two-port models for two modes of excitations, known as oddand even-modes, as shown in Fig. 6(a) and 6(b), respectively [20]. Figure 7 demonstrates the simulated frequency responses (S<sub>21</sub>) to which it can be seen that the asymmetrical parallelcoupled line has notch responses. The odd- and even- mode notches appear at the frequencies of 6.36 GHz and 6.0 GHz,

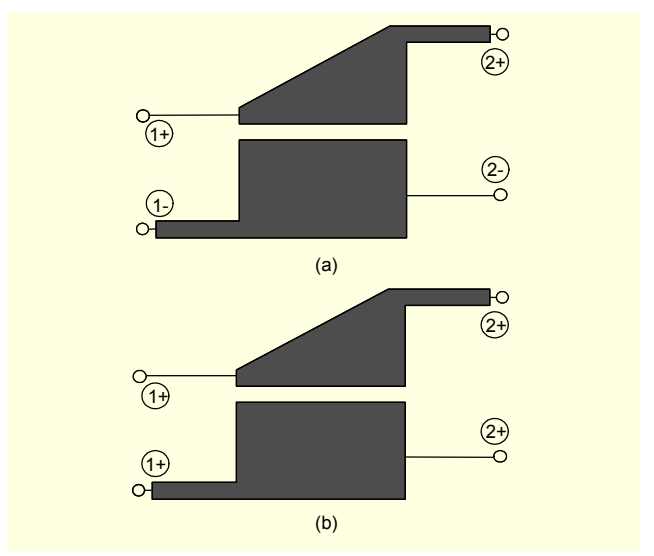


Fig. 6. The loading capacitance part of the proposed resonator forming an asymmetrical parallel-coupled line and modeled as an IE3D differential two-port for (a) odd- and (b) even-mode excitations.

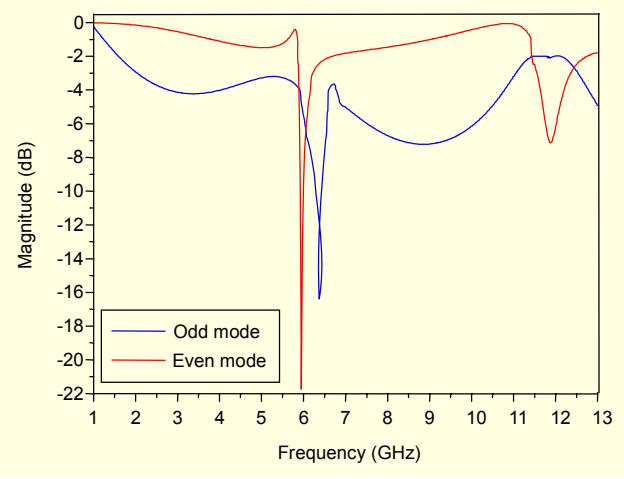


Fig. 7. Frequency responses  $(S_{21})$  of the asymmetrical parallel-coupled line with odd- and even-mode excitations.

respectively, closed to the first spurious response frequency of the proposed resonator. These odd- and even-mode responses will certainly affect the resonator, resulting in a bandstop characteristic; therefore, superior suppression of the first spurious response may be obtained.

#### IV. Filter Design and Measured Results

#### 1. Coupling Structures

The IE3D simulator, which is based on the method of moments which proves to be quite accurate in its prediction, was used to simulate the frequency responses of the three basic coupling structures. The coupling in each structure can be specified by the two dominant resonance frequencies, which are split off from the resonance condition due to the electromagnetic coupling. The coupling coefficients  $M_{ij}$  for resonators i and j would then be extracted from the simulated frequency responses by using [15].

$$M_{ij} = \pm \frac{f_2^2 - f_1^2}{f_2^2 + f_1^2},\tag{2}$$

where  $f_1$  or  $f_2$  corresponds to either even- or odd-mode resonance frequency. The external quality factor may be characterized by

$$Q_e = \frac{f_0}{f_{3dB}} \quad , \tag{3}$$

where  $f_0$  and  $f_{3dB}$  are the resonance frequency and 3 dB bandwidth of the input or output resonator when it alone is externally excited. The layouts of the two-resonator and four-resonator bandpass filters using the proposed microstrip slow-wave open-loop resonators and  $0^{\circ}$  feed structures, of which the signals at the input and output are in phase, are shown in Fig. 8 and Fig. 11, respectively.

#### 2. Two-Resonator Bandpass Filter

The first filter is an example of a two-resonator bandpass filter, which consists of the proposed microstrip slow—wave open-loop resonators. The filter was then fabricated on an RT/Duroid 3003 substrate with a relative dielectric constant of 3 and a thickness of 1.524 mm. In order to have a maximally flat passband bandwidth of 60 MHz (or the fractional bandwidth of FBW=3%) at  $f_0$  equal to 2 GHz, the external quality factor  $Q_e$  and the coefficient  $M_{2l}$  were calculated as

$$Q_e = \frac{c_0 c_1}{FBW} = 47.1, \tag{4}$$

$$M_{21} = -\frac{FBW}{\sqrt{c_1 c_2}} = -0.021,$$
 (5)

where  $c_0$ ,  $c_1$ , and  $c_2$  are element values. The spacing  $S_{12}$  between the resonators in Fig. 8 was adjusted to obtain the appropriate external quality factor and coupling coefficient with the aid of an IE3D EM simulator [16]. The filter parameters were obtained in the following:  $L_1 = 7$  mm,  $L_2 = 0.5$  mm,  $L_3 = 4.25$  mm,  $L_4 = 9$  mm,  $L_5 = 9$  mm, G = 0.5 mm, and W = 0.5 mm, with spacing  $S_{12}$  equal to 1.12 mm.

Figure 9 shows a photograph of the fabricated filter. The size of this two-resonator filter is about  $0.095\lambda_{go}$  by  $0.202\lambda_{go}$ , where

 $\lambda_{go}$  is the guided wavelength of a 50- $\Omega$  line on this substrate at the center frequency. The fabricated filter was then measured on an Agilent 8719ES network analyzer, with the measured and theoretical performance as shown in Fig.10. Figure 10(a) gives the details of the passband response. Due to the 0° feed structure, we can notice the appearance of two transmission zeros near the passband [14]. Figure 10(b) shows the wideband response. We can notice that the measured result shows a slight deviation in the center frequency and bandwidth. Also from the measured data, we found that the passband insertion loss is approximately 2.5 dB at the center frequency of 2.03 GHz, which is mainly due to the conductor loss of copper. The passband insertion loss curve of the proposed bandpass filter is sharper than that of the conventional filter. The passband return loss is greater than 20 dB and the out-of-band rejection is better than 20 dB at the lower stopband and 20 dB at the upper stopband. The two transmission zeros are at 1.91 GHz with 42 dB rejection and 2.13 GHz with 31 dB rejection, respectively. The filter exhibits a wide upper stopband with a rejection better than 20 dB up to about 10 GHz, and the first spurious response

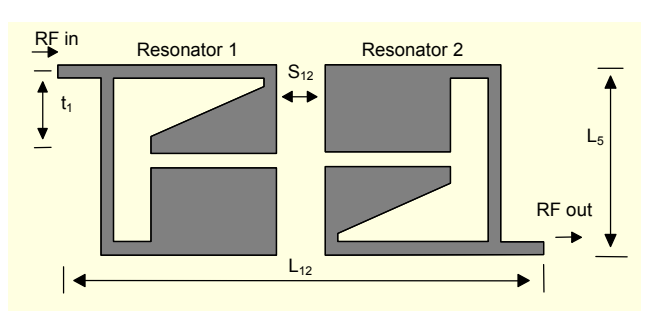


Fig. 8. Layout of the two-resonator designed filters with  $L_1 = 7$  mm,  $L_2 = 0.5$  mm,  $L_3 = 4.25$  mm,  $L_4 = 9$  mm,  $L_5 = 9$  mm, W = 0.5 mm, G = 0.5mm,  $L_{12} = 27.62$  mm, and  $t_1 = 4$  mm.

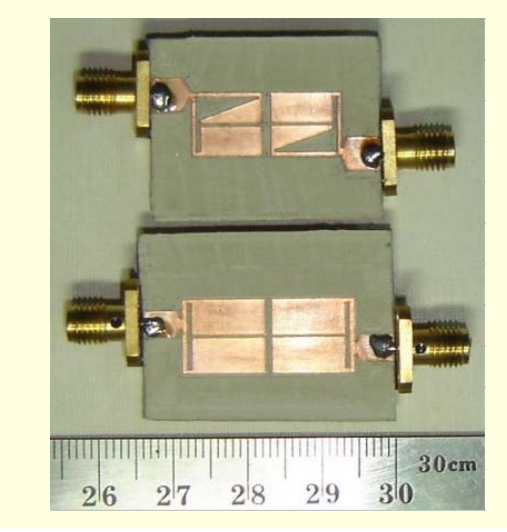


Fig. 9. A photograph of the proposed filter (top) and conventional filter (bottom).

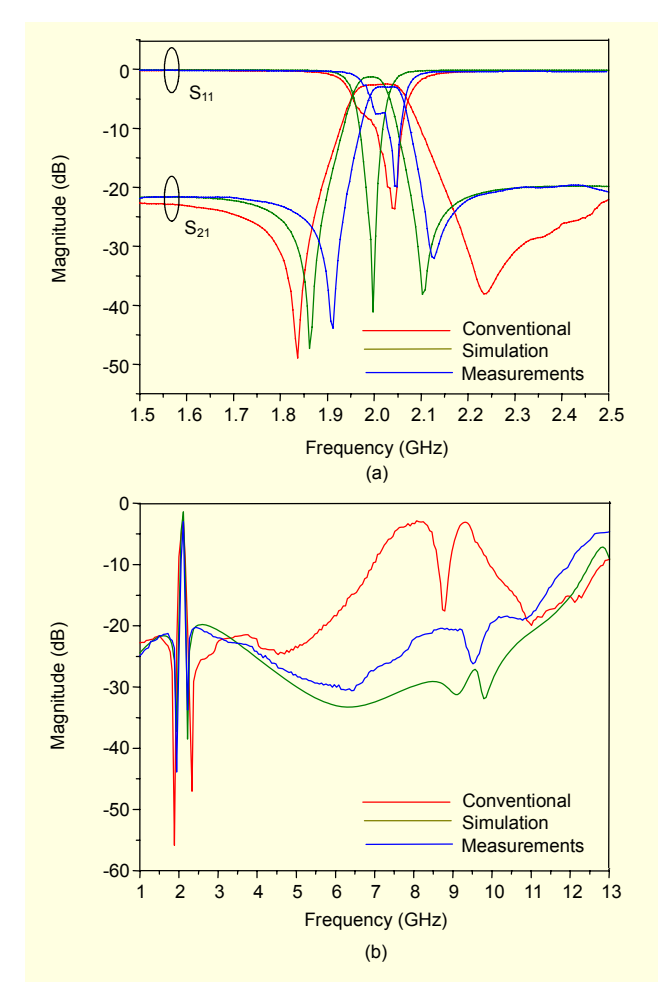


Fig. 10. Comparison of measured and simulated responses of the two-resonator slow-wave open-loop resonator filters' (a) passband response and (b) wideband response.

is about 6 dB at 12.7 GHz. The first spurious frequency is higher compared with the conventional structure because of the higher dispersion effect of the loading capacitance [15].

#### 3. Four-Resonator Cross-Coupled Filter

The second filter is an example of a four-resonator cross-coupled microstrip slow-wave open-loop resonator filter, designed and fabricated on the same microwave substrate and same resonator size of the designed two-resonator filter. The configuration of a four-resonator cross-coupled microstrip slow-wave open-loop resonator filter is shown in Fig. 11(a). Figure 11(b) shows the typical coupling structure of the four-resonator cross-coupled bandpass filter, where each node represents a resonator. The solid line and dotted line represent the direct coupling route and the cross-coupling route, respectively. The filter specifications are the center frequency of 2 GHz, a passband ripple of 0.01 dB, and the passband bandwidth of 60 MHz.

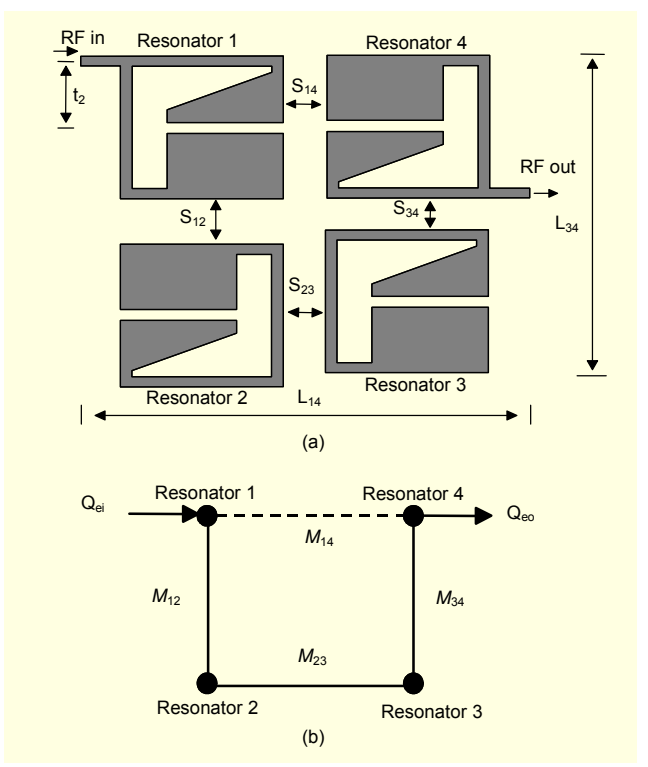


Fig. 11. (a) Layout of the four-resonator designed filters with  $L_1 = 7$  mm,  $L_2 = 0.5$  mm,  $L_3 = 4.25$  mm,  $L_4 = 9$  mm,  $L_5 = 9$  mm, W = 0.5 mm, G = 0.5 mm,  $S_{14} = 1.25$  mm,  $S_{23} = 1.5$  mm,  $S_{34} = 1.62$  mm,  $S_{12} = 2.75$  mm,  $L_{34} = 20.75$  mm,  $L_{14} = 28$  mm, and  $t_2 = 4$  mm. (b) Typical coupling structure.

The filter could be synthesized by using a method described in [22], from which the lumped-element values of a low pass prototype were determined as  $c_0 = 1$ ,  $c_1 = 0.95947$ ,  $c_2 = 1.42292$ ,  $J_1=-0.21083$ , and  $J_2 = 1.11769$ . The design parameters of the bandpass filter (namely, the elements of the coupling matrix and the input/output single-loaded external  $Q_e$ ) could then be calculated as

$$M_{12} = M_{34} = \frac{FBW}{\sqrt{c_1 c_2}} = 0.025,$$
 (6)

$$M_{23} = \frac{FBW \cdot J_2}{c_2} = 0.023 \,, \tag{7}$$

$$M_{14} = \frac{FBW \cdot J_1}{c_1} = -0.006 , \qquad (8)$$

$$Q_e = \frac{c_0 c_1}{FBW} = 31.99. (9)$$

The filter design is based on knowledge of the coupling coefficients of the three basic coupling structures, which are electric, magnetic, and mixed coupling, as described in [15]; therefore, the offset between resonators 2 and 3 is 1.25 mm. The

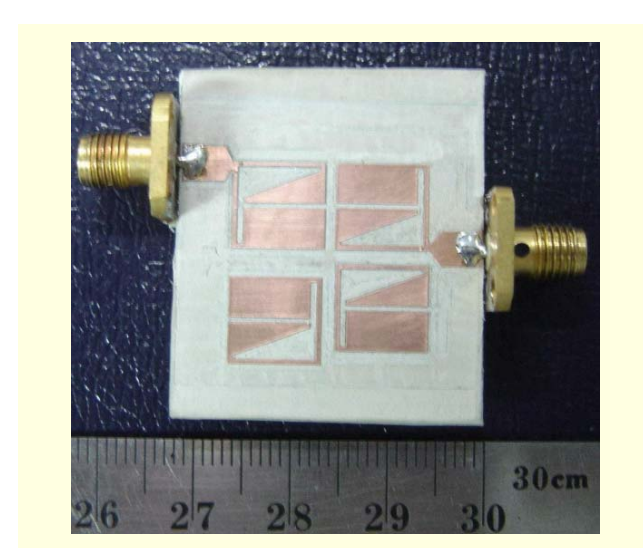


Fig. 12. A photograph of the fabricated four-resonator bandpass filter using the proposed microstrip slow-wave open-loop.

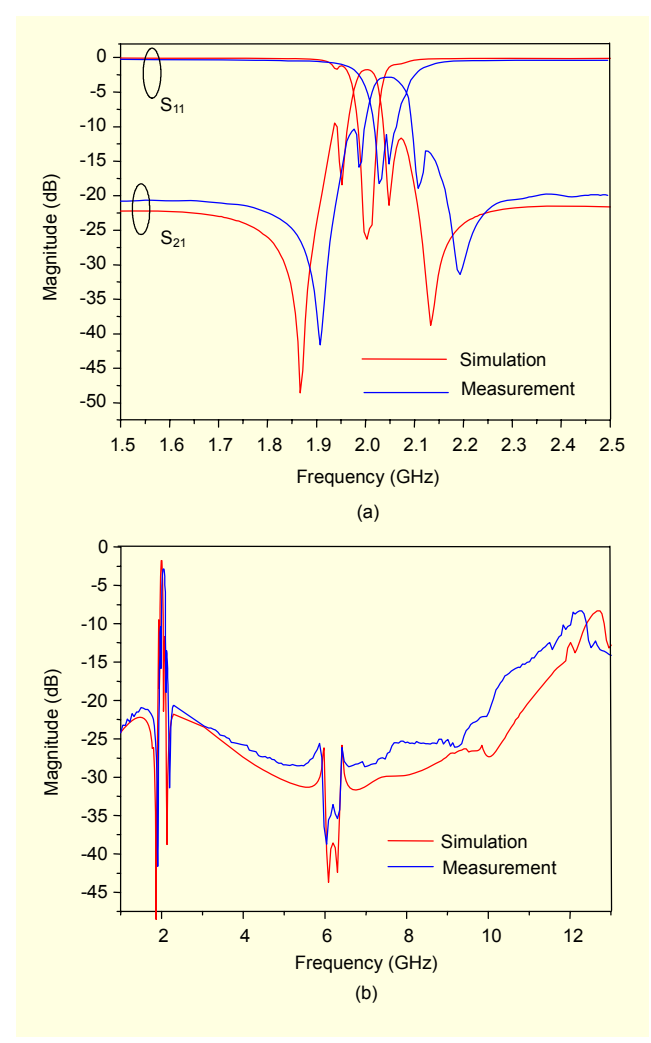


Fig. 13. Comparison of measured and simulated responses of the four-resonator slow-wave open-loop resonator filter (a) passband response and (b) wideband response.

spacing between the resonators in Fig. 11(a) has been determined as the following:  $S_{14} = 1.25$  mm,  $S_{23} = 1.5$  mm,  $S_{34} = 1.62$  mm, and  $S_{12}= 2.75$  mm. Figure 12 shows a photograph of the fabricated four-resonator bandpass filter using new microstrip slow-wave open-loop resonators. In this case, the size of the filter is only  $0.219\lambda_{go}$  by  $0.206\lambda_{go}$ . Figure 13(a) shows the measured and theoretical data. It can be expected that there is a single pair of transmission zeros near the passband due to the cross-coupling effect. The effect of the two transmission zeros at 1.98 GHz and 2.09 GHz is observed. It can be also clearly observed that there are two extra transmission zeros on opposite sides of the passband due to the 0° feed structure. One of the extra transmission zeros is at 1.93 GHz and the other is at 2.21 GHz. The measured passband insertion loss is approximately 2.78 dB at the center frequency of 2.05 GHz, which again is attributed to the conductor loss of copper. The passband return loss is greater than 18 dB. The out-of-band rejection is better than 22 dB at the lower stopband and 20 dB at the upper stopband. In Fig. 13(b), the filter exhibits a wide upper stopband with a rejection better than 25 dB up to about 10.5 GHz. It can also be clearly seen that there is an unnatural dip in the response at  $f_l$  around 6 GHz. The reason for this dip is that the bandstop characteristic of the asymmetrical parallel coupled-line of the proposed resonator causes superior suppression of the spurious response as previously discussed.

#### V. Conclusions

We have presented two bandpass filters designed using the proposed microstrip slow-wave open-loop resonators. The size of the resonators has been optimized from the standpoint of the resonators' unload Q-factor. These bandpass filters have been designed at an operating frequency of about 2 GHz and a bandwidth of 60 MHz. The filters are not only compact in the size, but also have a wider upper stopband as a result of the asymmetrical parallel-coupled line section of the proposed resonator. The measured responses have very good agreement with our simulation expectations.

#### References

- [1] I.C. Hunter, L. Billonet, B. Jarry, and P. Guillon, "Microwave Filters - Applications and Technology," *IEEE Trans. Microwave Theory Tech.*, vol. 50, no. 3, Mar. 2002, pp. 794-805.
- [2] Z. Ma, T. Kawaguchi, and Y. Kobayashi, "Miniaturized High-Temperature Superconductor Bandpass Filters Using Microstrip S-Type Spiral Resonators," *IEICE Trans. Electron.*, vol. E88-C, no. 1, Jan. 2005, pp. 57-61.

- [3] G. Zhang, F. Huang, and M.J. Lancaster, "Superconducting Spiral Filters with Quasi-elliptic Characteristic for Radio Astronomy," *IEEE Trans. Microwave Theory Tech.*, vol. 53, no. 3, Mar. 2005, pp. 947-951.
- [4] G. Tsuzuki, M. Suzuki, and N. Sakakibara, "Superconducting Filter for IMT-2000 Band," *IEEE Trans. Microwave Theory Tech.*, vol. 48, no. 12, Dec. 2000, pp. 2519-2525.
- [5] J.S. Hong, M.J. Lancaster, D. Jedamzik, R.B. Greed, and J.C. Mage, "On the Performance of HTS Microstrip Quasi-elliptic Function Filters for Mobile Communications Application," *IEEE Trans. Microwave Theory Tech.*, vol. 48, no. 7, July 2000, pp. 1240-1246.
- [6] G.C. Liang, D. Zhang, C.F. Shih, M.E. Johansson, R.S. Withers, D.E. Oates, A.C. Anderson, P. Polakos, P. Mankiewich, E.D. Obaldia, and R.E. Miller, "High-Power HTS m\Microstrip Filters for Wireless Communication," *IEEE Trans. Microwave Theory Tech.*, vol. 43, no. 12, Dec. 1995, pp. 3020-3029.
- [7] J.T. Kuo, S.P. Chen, and M. Jiang, "Parallel-Coupled Microstrip Filters with Over-Coupled End Stages for Suppression of Spurious Responses," *IEEE Microwave Wireless Compon. Lett.*, vol. 13, no. 10, Oct. 2003, pp. 440-442.
- [8] T. Lopetegi, M.A.G. Laso, J. Hernandez, M. Bacicoa, D. Benito, M.J. Garde, M. Sorolla, and M. Guglielmi, "New Microstrip 'Wiggly-Line' Filters with Spurious Passband Suppression," *IEEE Trans. Microwave Theory Tech.*, vol. 49, no. 9, Sep. 2001, pp. 1593-1598.
- [9] M.D. Castillo, V. Ahumada, J. Martel, and F. Medina, "Parallel Coupled Microstrip Filters with Ground-Plane Aperture for Spurious Band Suppression and Enhanced Coupling," *IEEE Trans. Microwave Theory Tech.*, vol. 52, no. 3, Mar. 2004, pp. 1082-1086.
- [10] M.D. Castillo, V. Ahumada, J. Martel, and F. Medina, "Parallel Coupled Microstrip Filters with Floating Ground-Plane Conductor for Spurious Band Suppression," *IEEE Trans. Microwave Theory Tech.*, vol. 53, no. 8, May 2005, pp. 1823-1828
- [11] J.T. Kuo, M. Jiang, and H.J. Chang, "Design of Parallel-Coupled Microstrip Filters with Suppression of Spurious Resonances Using Substrate Suspension," *IEEE Trans. Microwave Theory Tech.*, vol. 52, no. 1, Jan. 2004, pp. 83-89.
- [12] J.T. Kuo and E. Shih, "Microstrip Stepped Impedance Resonator Bandpass Filter with an Extended Optimal Rejection Bandwidth," *IEEE Trans. Microwave Theory Tech.*, vol. 51, no. 5, May 2003, pp. 1554-1559.
- [13] M. Makimoto and S. Yamasashita, "Bandpass Filters Using Parallel Coupled Stripline Stepped Impedance Resonators," *IEEE Trans. Microwave Theory Tech.*, vol. MTT-28, Dec. 1980, pp. 1413-1417.
- [14] S.Y. Lee and C.M. Tsai, "New Cross-Coupled Filter Design Using Improved Hairpin Resonators," *IEEE Trans. Microwave*

- Theory Tech., vol. 48, no. 12, Dec. 2000, pp. 2482-2490.
- [15] J.S. Hong and M.J. Lancaster, "Theory and Experiment of Novel Microstrip Slow-Wave Open-Loop Resonator Filters," *IEEE Trans. Microwave Theory Tech.*, vol. 45, no. 12, Dec. 1997, pp. 2358-2356.
- [16] S. Oh and Y. Kim, "A Compact Bandpass Filter Using Microstrip Slow-Wave Open-Loop Resonators with High Impedance Line," *Microwave and Optical Tech. Lett.*, vol. 38, no. 3, Aug. 2003, pp. 185-187.
- [17] R. Levy, "Filters with Single Transmission Zeros at Real or Imaginary Frequencies," *IEEE Trans. Microwave Theory Tech.*, vol. MTT-24, Apr. 1976, pp. 172-181.
- [18] J.S. Hong and M.J. Lancaster, "Couplings of Microstrip Square Open-Loop Resonators for Cross-Coupled Planar Microwave Filters," *IEEE Trans. Microwave Theory Tech.*, vol. 44, no. 12, Dec. 1996, pp. 2099-2109.
- [19] J.S. Hong and M.J. Lancaster, "Design of Highly Selective Microstrip Bandpass Filters with a Single Pair of Attenuation Poles at Finite Frequencies," *IEEE Trans. Microwave Theory and Tech.*, vol. 48, no. 7, July 2000, pp. 1098-1107.
- [20] Zeland Software, Inc., IE3D, NewYork.
- [21] L.H. Hsieh and K. Chang, "Equivalent Lumped Elements G, L, C, and Unloaded Q's of Closed- and Open-Loop Ring Resonators," IEEE Trans. Microwave Theory Tech., vol. 50, no. 2, Feb. 2002, pp. 453-459.



**Prayoot Akkaraekthalin** received the B.Eng. and M.Eng. degrees in electrical engineering from King Mongkut's Institute of Technology, North Bangkok (KMITNB), Thailand, in 1986 and 1990, respectively, and the PhD degree in electrical engineering from the University of Delaware, Newark, USA, in 1998. From 1986

to 1988, he worked in the Microtek Laboratory, Thailand, as a Research and Development Engineer. In 1988, he joined the Department of Electrical Engineering, KMITNB, as an Instructor. His research interests are in the areas of microwave circuit design, optoelectronics and telecommunications.



Jaruek Jantree received the B.Eng. degree in electrical engineering from Rajamangala Institute of Technology (RIT), Krong 6, Thailand, in 1997, and the M.Eng. degree in electrical engineering from King Mongkut's Institute of Technology North Bangkok (KMITNB), Thailand, in 2001. He is now

pursuing the PhD degree in electrical engineering at KMITNB. His research interest is in the area of microwave circuit design.